Development of New Fluorescent Molecules for use as Biomolecular Probes

By

Murali Paranjothy

Department of Chemistry and Biomolecular Sciences

Macquarie University

This thesis is submitted in fulfilment of requirements for the degree of

Master of Research (MRes)

8th of May 2015

Supervisor: Assoc. Prof. Andrew Try

Acknowledgements

It would be my pleasure to thank the following people who helped in making this thesis possible.

I offer my profound gratitude to my supervisor Associate Professor Andrew C Try. With his patience, enthusiasm, energy and great efforts to explain things clearly to me, he made learning chemistry a fun and enjoyable experience for me. Throughout the period of my MRes, he provided encouragement, good teaching and good company in performing the research experiments.

I am very much thankful to Dr. Nima Sayyadi, a Post-doctoral fellow, for his valuable time, help and guidance for performing initial synthetic and final imaging experiments.

I am deeply grateful to Dr. Andrew Care, a Post-doctoral fellow, for his helpful nature, guidance, support and his ideas in designing the biological experiments.

I express my sincere gratitude to thank Dr. Anwar Sunna and Dr. Russell Connally for their trust in me and providing the necessary facilities for performing the experiments.

I convey my sincere thanks to my fellow group mates Imam, Mohammed, Michael, Rashid, Masoud and Rajesh for their valuable time and sharing their expertise with me.

I would like to thank my fellow friends Ketan, Karthik, Aneesh, Jashn, Ishan and Irene Justiniano from ASAM for their help and support in finishing my final experiments.

I wish to express my sincere thanks to the MRes committee members Assoc. Prof. Bridget Mabbutt, Dr. Louise Brown and Prof. Mark Molloy for their constant support and encouragement.

I take this opportunity to thank various members of the department of CBMS, including Ryan and Harry for their encouragement and I also thank the Karuso group and Danny's group for their kind advice, assistance in materials supply when needed and instrumental operating skills, and Anthony Gurlica for his assistance in laboratory practice.

Last but not least, I convey my gratitude to my Amma, Appa, Chitti, Chitappa, my brothers Pradeep and Vibin, my cousins, my family members, friends back home and the almighty for their trust in me and their constant support.

Declaration

I certify that in this work entitled "Development of New Fluorescent Molecules for use as Biomolecular Probes" has not been previously submitted as part of requirements for a degree to any other university or institution other than Macquarie University. I also certify that the thesis is an original piece of research and it has been written by me. Any help and assistance that I have received in my research work and the preparation of the thesis itself have been appropriately acknowledged. Finally, I certify that all information sources and literature used are indicated in the thesis.

Murali Paranjothy

(SN: 43574440)

08/05/2015

Abstract

This thesis is composed of two aspects of research that will be linked as part of a future PhD project.

The first part describes the development of two new ligands designed to chelate lanthanide ions – specifically europium and terbium. The ligands are based on the known terphenyl platform (and are related to BHHCT), but replace the central phenyl ring with a 2,3-disubstituted quinoxaline ring. The goal of this aspect of the research is to prepare compounds capable of producing long-lived fluorescence that is either red (for Eu^{3+} chelates) or green (for Tb^{3+} chelates) that can be conjugated to biomolecules to form biological probes.

The second part is aimed at preparing a fluorescent peptide conjugate from a linker peptide (LPG) with conventional fluorescent dyes from the Alexa Fluor family. The ability of this conjugate to directly label an antibody to quickly and efficiently generate a fluorescent antibody for use as a biomolecular probe was also investigated.

Utimately, the new lanthanide chelates described in the first part of this work will be covalently bound to Linker Protein G (LPG). LPG is a recombinant fusion protein consisting of two regions; (a) a peptide linker sequence containing eight lysine residues and (b), *Streptococcus* Protein G' which has specific binding affinity towards antibodies. The lanthanide chelates will be attached to LPG *via* the lysine residues in the linker region, and the assembly will interact with target antibodies via the Protein G binding region, to afford antibodies labelled with a long-lived fluorescence probe that can be visualised with time-gated techniques.

List of Abbreviations and Symbols

°	degrees
Ac	acetyl
app	apparent
aq	aqueous
b.p	boiling point
Bn	benzyl
br	broad
$CDCl_3$	chloroform-*d*
°C	degrees Celsius
δ	NMR chemical shift in parts per million
d	doublet
dd	doublet of doublets
DCM	dichloromethane
DME	dimethoxyethane
DMF	*N*,*N*-dimethylformamide
DMSO	dimethylsulfoxide
DMSO-d_6	dimethylsulfoxide-d_6
EtOH	ethanol
Et	ethyl
g	gram
h	hour
Hz	hertz
J	coupling constant
LPG	linker protein G
Me	methyl
mg	milligram
min	minute
mmol	millimole
µ	micro
NHS	*N*-hydroxysuccinimide
NMR	Nuclear magnetic resonance

nmol	nanomol
OD600	optical density at 600 nm
PG	protein G
Ph	phenyl
pmol	picomole
ppm	parts per million
q	quartet
R	any functional group
rt	room temperature
s	singlet
t	triplet
TLC	Thin layer chromatography
UV	ultra-violet

Table of Contents

Chapter One Introduction

1.1 The Fluorescence Process

Fluorescence is the product of a three-stage process that occurs in certain molecules; this involves absorption, then excitation, internal conversion and emission. The process responsible for fluorescence is depicted by an electronic-state diagram (Jablonski diagram) as shown in Figure 1.1.

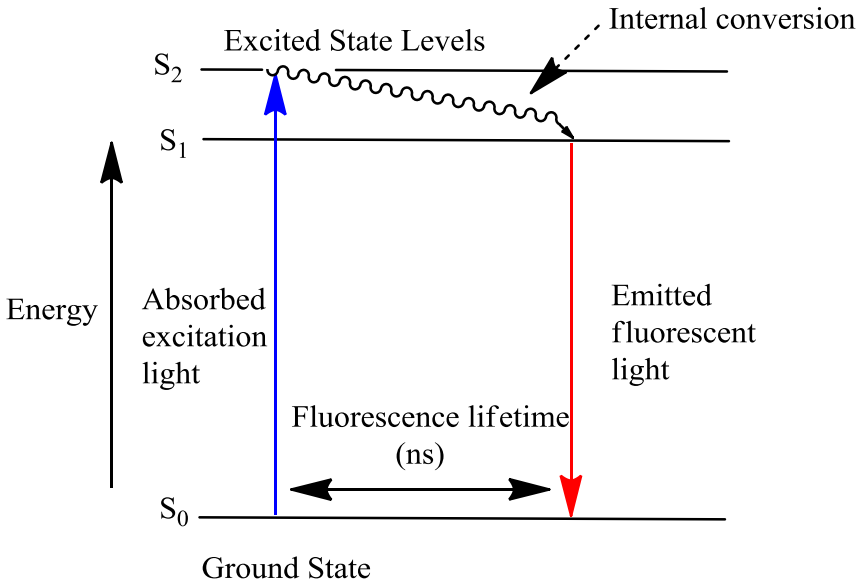

Figure 1.1: Jablonski energy diagram of the electronic transitions associated fluorescence (adapted from Zimmermann *et al.*).[1]

Typically, a fluorophore is excited by the absorption of a photon of energy. This absorption of energy usually excites the fluorophore from the ground state depicted as S_0 to a higher electronic state such as S_1 or S_2. After excitation, the fluorophore only exists in the excited state for a finite time, during which it typically undergoes conformational change. This change causes the energy in the excited electronic singlet state to partially dissipate and creates a relaxed singlet electronic excited state in the lowest vibrational level S_1, represented as Internal Conversion (IC). The final step of fluorescence is emission. The photon of energy is emitted, returning the fluorophore to the ground state and creating the phenomenon known as fluorescence.[1]

The phenomenon of fluorescence has been used in biological research for over 100 years, although developments in fluorescence chemistry, along with technical discoveries, have fuelled the development of many different kinds of fluorophores (a compound, or part of a compound, that exhibits fluorescent properties). In the past 70 years the phenomena of

fluorescence has evolved from a scientific interest into an essential tool with utility in various research fields and applications covering many facets of science.[2]

1.2 Features of Fluorescence Spectra

Both the excitation and emission wavelengths are specific characteristics for each fluorophore, and while these wavelengths are discrete for monoatomic fluorophores, polyatomic fluorophores can exhibit broad excitation and emission spectra. It is important to note that while the emission wavelength is generally independent of the excitation wavelength due to partial loss of energy prior to emission, the emission intensity is proportional to the amplitude (intensity) of the excitation wavelength, as indicated by the excitation energies (Ex_1 and Ex_2) and their corresponding emission intensities (Em_1 and Em_2, respectively, as shown in Figure 1.2.

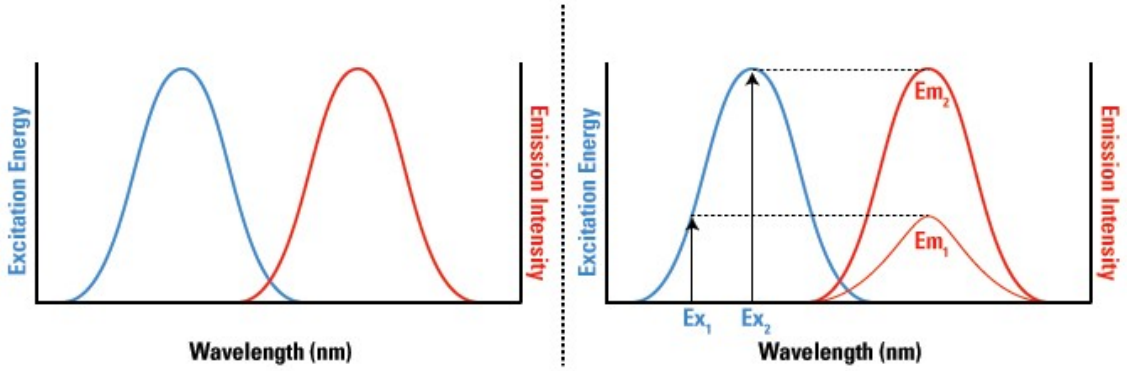

Figure 1.2: (a) Schematic absorption (blue) and emission (red) peaks. (b) Schematic of the effect on the intensity of the emission band in relation to different intensities of excitation energy.

The distance between the excitation and emission wavelengths is called the Stokes Shift (Figure 1.3) and is a key aspect in the detection of the emitted fluorescence in biological applications. The Stokes shift is also a distinct characteristic of each fluorophore. For example, fluorophores with large Stokes shifts (Figure 1.3(a)) are easy to distinguish because of the large separation between the excitation and emission wavelengths. On the other hand, the detection of emitted fluorescence can be difficult to distinguish from the excitation light when using fluorophores with very small Stokes shifts (Figure 1.3(b)), because the excitation and emission wavelengths have a significant overlap, and the fluorescence is essentially quenched by the "reabsorbance" of the emitted light. The Stokes shift is especially critical in multiplex fluorescence applications (where different coloured fluorophores are used

simultaneously), because the emission wavelength of one fluorophore may overlap, and therefore excite, another fluorophore in the same sample.

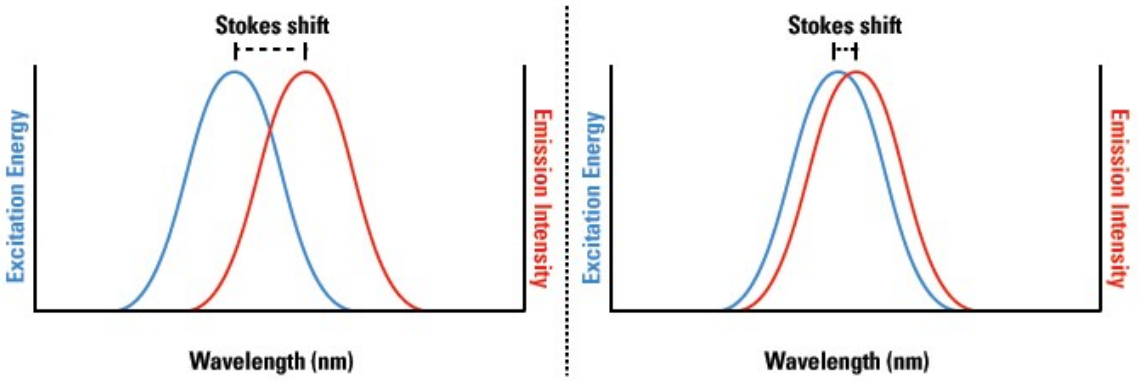

Figure 1.3: Schematic illustration of the excitation and emission profiles of a molecule with a favourable Stokes shift (left) and unfavourable (right). The larger the separation between the excitation and emission profiles, the better.

Another important parameter in fluorescence spectroscopy is the quantum yield. The fluorescence quantum yield is the number of emitted photons relative to the number of absorbed photons and is therefore a measure of the efficiency of the energy transferred from incident light to emitted fluorescence.[3] Substances with the largest quantum yields approaching unity, such as rhodamines (an example is shown in Figure 1.4), display the brightest emissions.[4] The sensitivity and selectivity required for fluorescence techniques are linked to the spectral properties and characteristics of fluorophores, and therefore the optimisation of the properties of new fluorophores through the use of synthetic organic chemistry is vital.

1.3 Types of Fluorophores

The vast selection of fluorophores commercially available today provides greater flexibility, variation and fluorophore performance for research applications than ever before. Fluorophores can be broadly divided into two main classes, intrinsic and extrinsic.[4] Intrinsic fluorophores are fluorescent natural products, for example some aromatic amino acids (such as tryptophan, tyrosine and phenylalanine), and some natural occurring pigments, such as chlorophyll. Extrinsic fluorophores are chemically synthesised fluorescent probes that are designed to provide fluorescence. Extrinsic fluorophores include fluorescein, rhodamine, BODIPYs and numerous others. The importance of extrinsic fluorophores is that many molecules of interest are non-fluorescent (such as in DNA and lipids), or else their naturally-

produced fluorescence is below a level of detection. In these cases, extrinsic fluorophores can be used to label these molecules. A range of fluorophores have been designed for this use and are available for both covalent and non-covalent labelling.[5] Some of the more widely used fluorophores are shown in Figure 1.4.

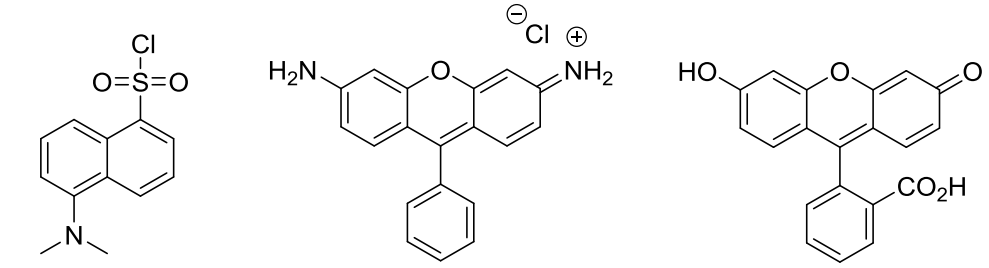

Dansyl chloride Rhodamine Fluorescein

Figure 1.4: Examples of some extrinsic fluorophore core structures.[4, 6][1]

A common use for both fluorescein and rhodamine is the labelling and detection of antibodies.[7] The small size of these fluorophores is a benefit over larger compounds for bioconjugation strategies because they can be cross-linked to macromolecules, such as antibodies, biotin or avidin, without interfering with proper biological function.

Indeed, modified versions of many simple fluorescent dyes are sold commercially as kits for the labelling of biological substrates. Alexa Fluor 488 (Figure 1.5) is a modified rhodamine molecule and is used in this project (see Section 2.5), with the *N*-hydroxysuccinimide (NHS) ester serving as an activated leaving group for attachment (conjugation) with substrates of interest, typically *via* reaction with amino groups on the molecules to be labelled.

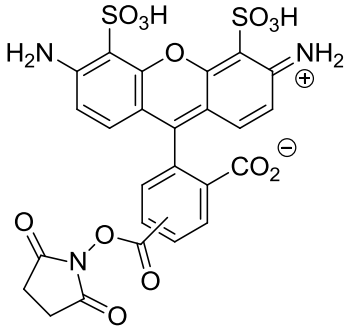

Figure 1.5: The structure of Alexa Fluor 488.

In recent years there has been a large interest in organic boron complexes as fluorophores, [8] with the most well-known being boron difluoride-dipyrromethene (BODIPY) dyes (the basic

framework is shown in Figure 1.6) which have now replaced fluorescein and rhodamine as extrinsic fluorophores for many applications.[9]

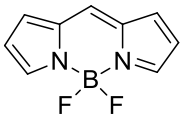

Figure 1.6: The core structure of an unsubstituted boron difluoride-dipyrromethene (BODIPY) 4,4-difluoro-4-bora-3a-4a-diaza-s-indacene.

The advantages of BODIPY include higher molar absorptivity, narrow absorption and emission bands and higher quantum yields. However, one major limitation of the BODIPY core is a small Stokes shift in the range of 400-600 cm^{-1}.[10]

A family of related compounds are boron difluoride complexes of 1,3-diketones ((1,3-diketonato)boron difluoride).

1.4 Boron Difluoride Complexes of 1,3-Diketones

Boron difluoride complexes of 1,3-diketones have been known for more than 90 years.[11] The core structure of a boron difluoride complex with 1,3-diketones contains a tetrahedral boron attached to the two oxygen atoms of a 1,3-diketone *via* co-ordination bonds (Figure 1.7). The six-membered ring containing the boron atom is isoelectronic with that found in BODIPY. Therefore, it is not surprising that boron difluoride complexes of appropriately functionalised 1,3-diketones often exhibit similar properties to those of BODIPY, including the ability to strongly absorb UV light and fluoresce with a high quantum yield.

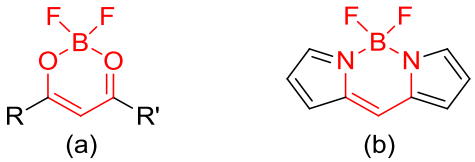

Figure 1.7: A figure highlighting the isoelectronic nature of (a) boron 1,3-diketone complexes and (b) BODIPY. Where R and R^1 = alkyl or aryl. In both case the organic ligand is bidentate and monoanionic.

1,3-Diketones are typically prepared by a variation on a general strategy (Claisen-like condensation), involving the attack of a nucleophilic α-carbon on the carbonyl group of a carboxylic acid derivative (eg acyl halide or methyl/ethyl ester). The nucleophilic α-carbon can be generated by treatment of a methyl ketone with either sodium hydride, sodium amide, or potassium *t*-butoxide, among others. Regardless of the choice of base, the solvent used in the reaction must be anhydrous to avoid the unwanted side reaction of ester/acyl halide

hydrolysis, that would result in the formation of unreactive carboxylate anions. 1,3-Diketonatoboron difluoride complexes can be prepared simply by treating a 1,3-diketone with boron trifluoride diethyl etherate. The complex is formed from the incorporation between the boron difluoride and the two oxygen atoms of a 1,3-diketone *via* a co-ordination bond (the ligand behaves as a mono-anionic bidentate chelator) (Scheme 1.1).

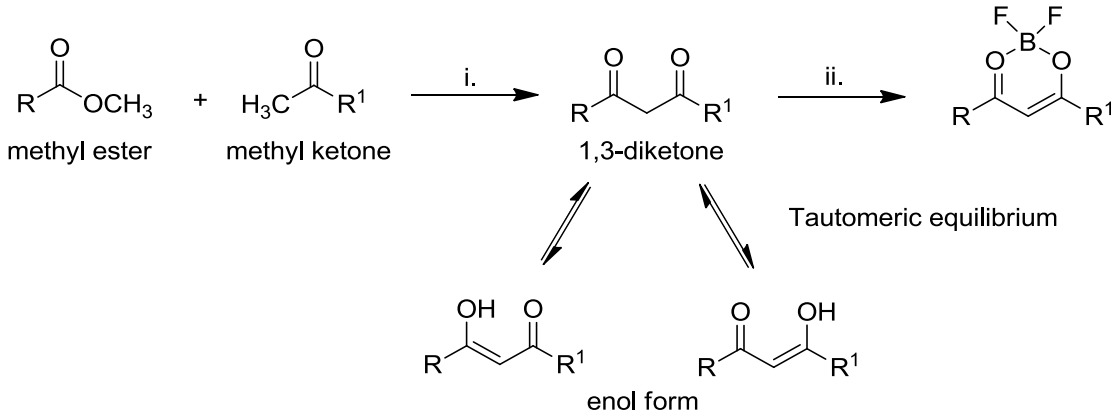

Scheme 1.1: i. NaH (or CH_3ONa), DME (or THF), reflux overnight. ii. $BF_3.OEt_2$, benzene (or DCM), reflux.

Note that 1,3-diketones exist in tautomeric equilibrium with their enol form(s), but the 1,3-diketone form is generally used in this thesis.

1.5 Long-Lived Fluorescence with Lanthanide Complexes

Another broad class of ligands that can be considered as a sub-class of the extrinsic fluorophore category, are those of lanthanide complexes, specifically Eu^{3+} and Tb^{3+}. The emission and absorption spectra of lanthanides ions consist of sharp and narrow bands which correspond to the Laporte-forbidden *f–f* transitions and are therefore weak in their absorption and emission intensities. However, this disadvantage can be overcome by indirect sensitization through the absorption bands (indirect excitation) of the ligand (or the "antenna" molecules) of appropriate complexes of the Ln(III) ions using UV light. An important aspect of these specially designed ligands is to maximize the protection of the Ln(III) ion from quenching, which involves the intrusion of solvent molecules (*eg* H_2O) into the inner sphere coordination of the metal ion. The luminescent properties of Ln(III) ions are hugely affected by the radiationless deactivation processes that occur upon coordination with OH, NH, and CH groups, due to vibration of the X-H bonds of the solvent.

The indirect sensitization is achieved as a sequence of steps involving the absorbance of light by the organic chromophore, followed by the intramolecular relay of energy from the ligand to the metal ion which results in the emission of light by the metal ion.[12] This process is shown schematically in Figure 1.8.

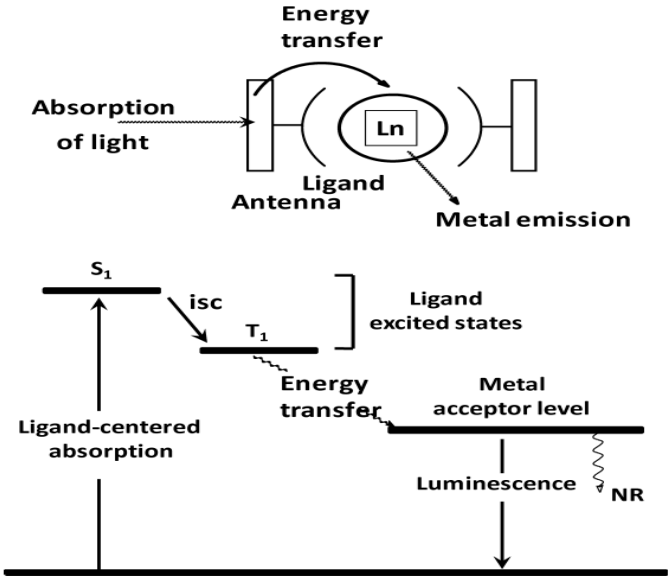

Figure 1.8: Simplified diagram explaining the indirect sensitization of lanthanide luminescence through the absorption bands of ligand molecules. (S_1 is the singlet state, T_1 is the triplet state, ISC is intersystem crossing and NR is non-radiative pathway).[13]

The easiest way to minimise these radiationless deactivations is to occupy the entire first coordination sphere with multidentate ligands such as those shown in Figure 1.9.

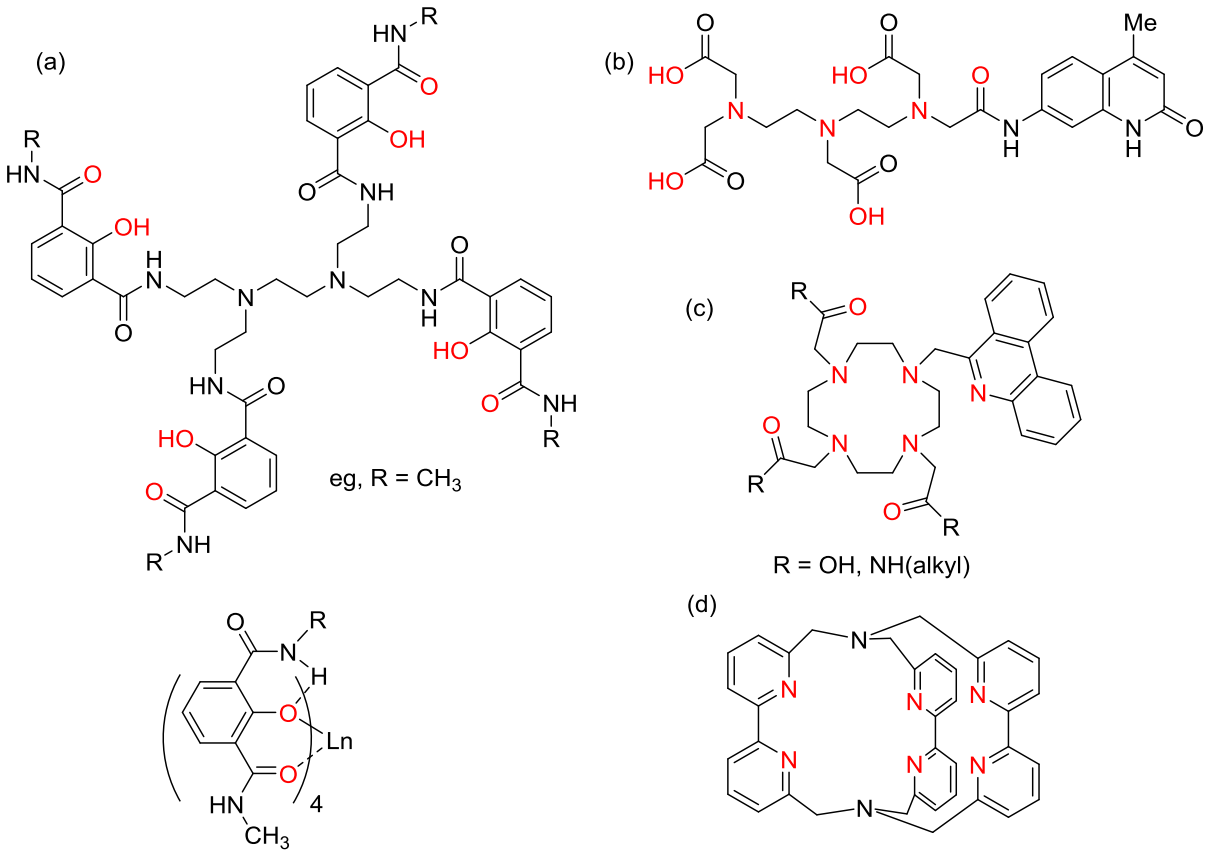

Figure 1.9: Some examples of ligands employed in the sensitization of Ln(III) ions. (a) 2-hydroxyisophthalamide ligand and schematic Ln complex from the Raymond group,[14] two pendant chromophore molecules linked to multidentate groups (b) from the Selvin group[15] and (c) the Parker group[16] and (d) a tris bipyridyl cryptand developed by Lehn and co-workers.[17]

1.6 BHHCT (4,4'-bis(l",1",l",2",2",3",3"-heptafluoro-4",6"-hexanedione-6"-yl)-chlorosulfo-*o*-terphenyl)

Of relevence to the current work, is the Eu^{3+} sensitizing ligand 4,4'-bis(l",1",l",2",2",3",3"-heptafluoro-4",6"-hexanedione-6"-yl)-chlorosulfo-*o*-terphenyl, commonly known as BHHCT (Figure 1.10(a)).[18] The sulfonyl chloride on BHHCT is used as a linking group to attach the ligand to a biomolecule of interest, generally *via* a reaction with an amino group present on the substrate. Note that the 1,3-diketones in these molecules exist in tautomeric equilibrium with their enol forms, as shown in Scheme 1.1, Section 1.4. The two 1,3-diketone arms form coordination bonds to lanthanide ions, and BHHCT therefore acts as a dianionic tetradentate ligand toward lanthanide(III) ions (Figure 1.10(b)).

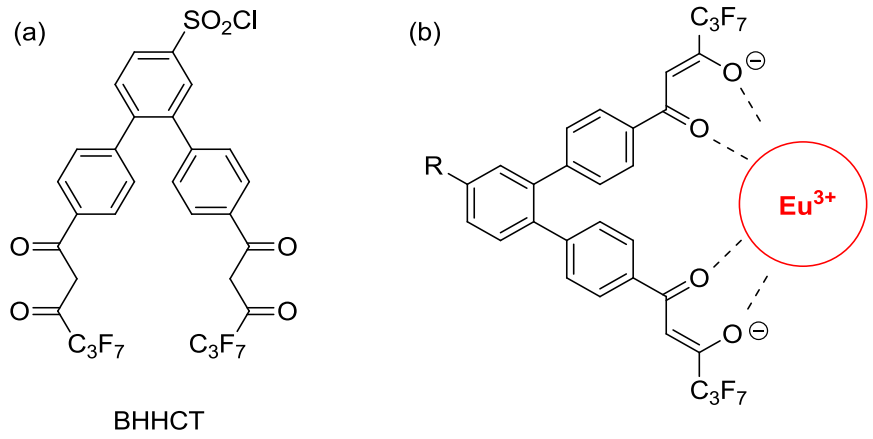

Figure 1.10: (a) The structure of BHHCT and (b) an illustration of the binding mode of the ligand to a europium ion.

In recent years, some other variations on the BHHCT molecule have been reported, and several of these are illustrated in Figure 1.11.[19]

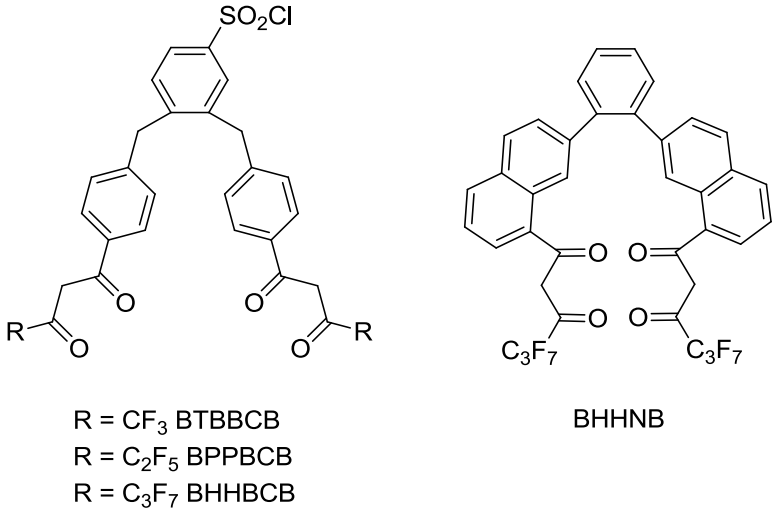

Figure 1.11: Two recently reported frameworks that are BHHCT analogues.

The inclusion of the methylene linkage between the aryl rings is reported to maximize the fluorescence intensity and quantum yield of Eu^{3+} complexes.[19c]

1.7 Project Aims

The role of this project is to scope suitable lines of research for a larger PhD project. As such, rather than focus on one aspect of a project and fully explore its limits, several projects were commenced in this work.

The aims of this Thesis were to:

i. Commence synthesis of fluorescent molecules that would ultimately afford analogues of BHHCT and BHHCB, as shown in Figure 1.12.

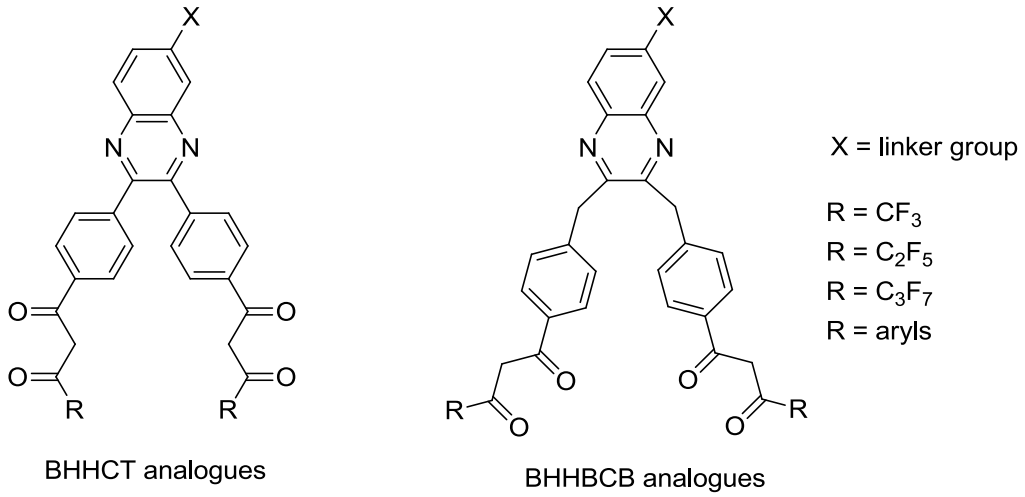

Figure 1.12: Two targeted classes of potential ligands for use in the preparation of fluorescent lanthanide complexes for use in the synthesis of labelled bioconjugates.

ii. Commence work on the methodology to permit the synthesis of a family of fluorescent peptide conjugates from linker peptide G (LPG) with conventional fluorescent dyes from the Alexa Fluor family, and ultimately new fluorescent lanthanide complexes.

iii. Investigate the ability of LPG-dye conjugates to directly label an antibody to quickly and efficiently generate a fluorescent antibody for use as a biomolecular probe.

Chapter Two Results and Discussion

2.1 Background

The various facets of this project are discussed below, and at the end of each section the short-term planned future work (as part of a PhD project) is briefly outlined.

As noted in Section 1.7, the project can broadly be divided into two sections, the first associated with synthetic chemistry, ultimately leading to the syntheses of fluorescent dye molecules and the second is preliminary work with the synthesis of conjugates of biological molecules with fluorescent dyes and the associated development of their use in assays.

Within the organic chemistry component, work was commenced in several areas; the syntheses of an analogue of BHHCT, with the central phenyl ring replaced with a quinoxaline ring system; a methylene linked analogue of BHHCT, again with the central phenyl ring replaced with a quinoxaline unit; some hydroxychalcone syntheses, for both boron and lanthanide chelation studies (with the expectation that, if formed, both types of complexes will exhibit fluorescent properties).

In the second part of this work, protein-dye conjugates were prepared, and together with a commericially available conjugate, these were use in an assay to visualise *Cryptosporidium oocysts*. These are important targets to visualize as they can cause diarrhea in humans when ingested in contaminated water, and the antibodies to the *Cryptosporidium oocysts* were readily available in the lab.

2.2 Synthesis of Quinoxalines

An initial target of this work was the synthesis of analogues of BHHCT in which the central benzene ring is replaced with a quinoxaline unit. The synthetic route to BHHCT is outlined in Scheme 2.1.

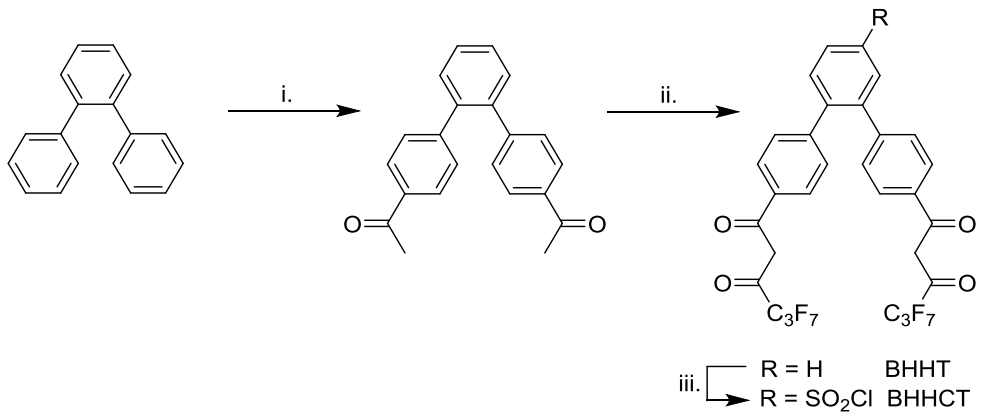

Scheme 2.1: i. AcCl, $AlCl_3$, CH_2Cl_2; ii. ethyl heptafluorobutyrate, NaOMe, THF; iii. $ClSO_3H$.

At the outset of this work two strategies toward the quinoxaline analogue of BHHCT were envisaged, with the only difference being the placement of the methyl ketone and the methyl ester groups, as shown in the retrosynthetic analysis in Figure 2.1.

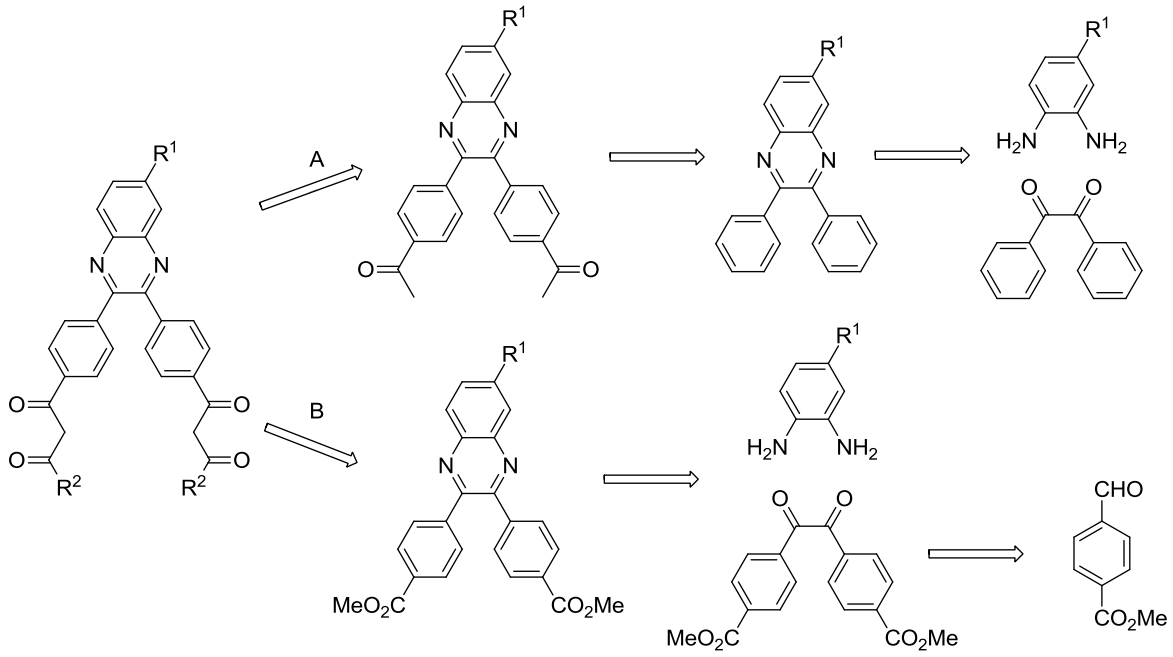

Figure 2.1: Retrosynthetic analysis of the quinoxaline analogue of BHHCT (R^1 = H or some functional group, R^2 may be aryl, heteroaryl, alkyl or fluoroalkyl).

Pathway A involved the methyl ketone being present on the phenyl rings of a 2,3-diphenylquinoxaline. This strategy closely resembled that taken in the synthesis of BHHCT and was the most efficient (in terms of the number of steps from commercially available starting materials). It was therefore the first to be examined.

Quinoxalines **1** and **2** were prepared by the condensation reaction of benzil with *o*-phenylenediamine or 1,2-diamino-4-nitrobenzene, as shown in Scheme 2.2.

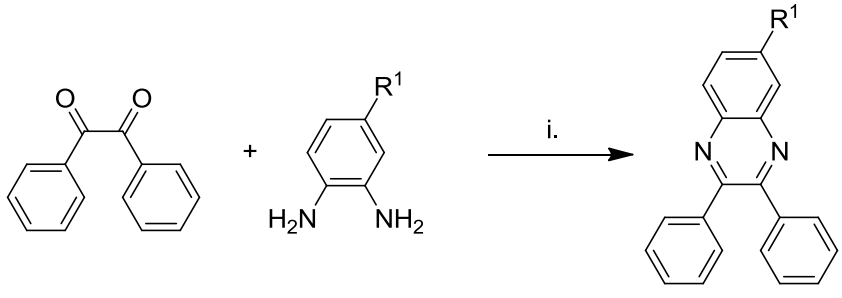

1 R = H 96%
2 R = NO_2 64%

Scheme 2.2: i. glacial acetic acid, reflux.

Compound **1** was to serve as a model compound, as it lacks a functional group handle for subsequent attachment to a substrate of interest, while the nitro group of **2** could be reduced to an amino group at a later stage in the synthesis, and then reacted with a linker molecules that could be used to bind to a biological substrate. The lower yield of **2** may be the result of the electron-withdrawing nitro group, or the reduced solubility of the compound in organic solvents (some intractable material was present during the work-up of the reaction), however each reaction was only performed once.

Prior to acetylation reactions being performed on **1** and **2**, *o*-terphenyl was used as a starting material in the reaction with acetyl chloride, using the conditions of Yuan *et al.*,[18a] to establish that the reagents and conditions to be employed on the new substrates were appropriate to afford the known compound **3** (Scheme 2.3).

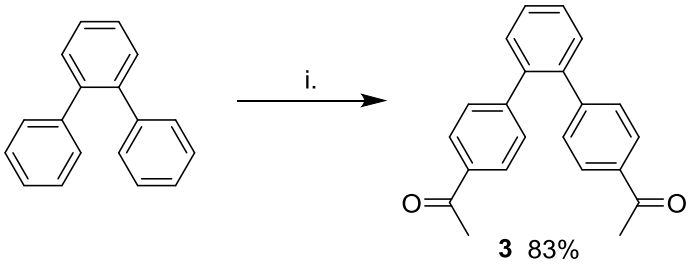

Scheme 2.3: i. AcCl, $AlCl_3$, CH_2Cl_2.

It is interesting that the acetylation of the central aryl ring of *o*-terphenyl (doubly activated toward electrophilic substitution reactions) is not a major product in this reaction, nor even a significant by-product. The structure of **3** was confirmed by examination of the ^{1}H NMR spectrum (Figure 2.2), with a signal integrating as six protons at δ 2.57 ppm (not shown) confirming bis-acetylation and the presence of an AB quartet, each component integrating as four protons, at δ 7.22 and 7.82 ppm confirming the site of acetylation.

Whilst **3** was successfully obtained, when either **1** or **2** were used as stating materials, they were recovered quantitatively, with no evidence of the formation of a new compound following TLC analysis of the reaction mixture prior to work up, or from ^{1}H NMR analysis after work-up.

Pathway B, Figure 2.1, was therefore investigated. This route commenced with the esterification of 4-formylbenzoic acid, followed by formation of the benzoin[20] **4** and subsequent oxidation to the substituted benzil[21] **5** (Scheme 2.4).

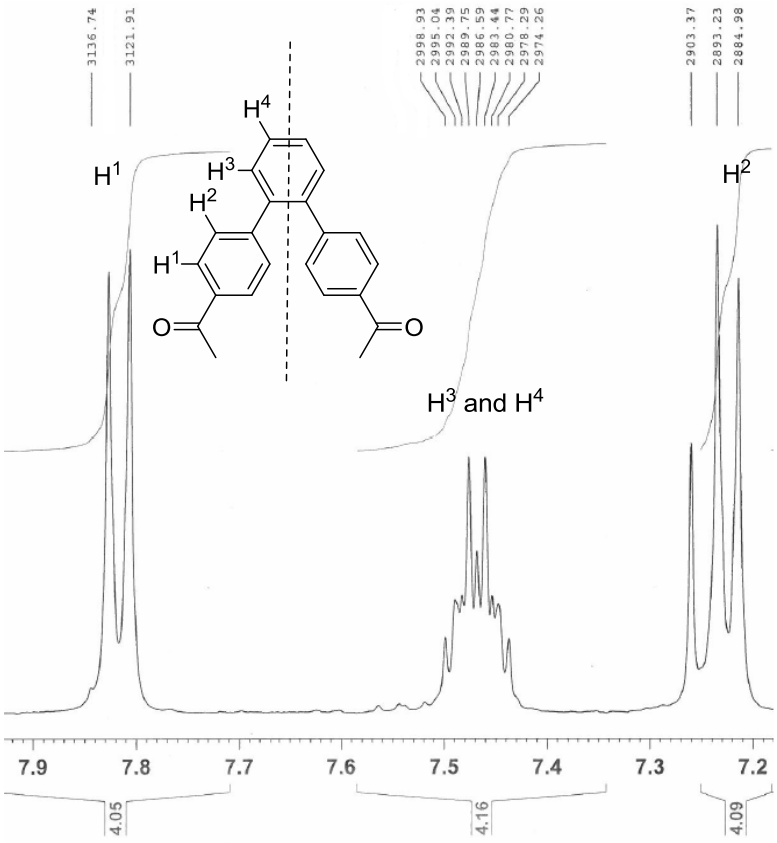

Figure 2.2: 400 MHz ^{1}H NMR spectrum ($CDCl_3$, 298 K) of the aromatic region of **3**.

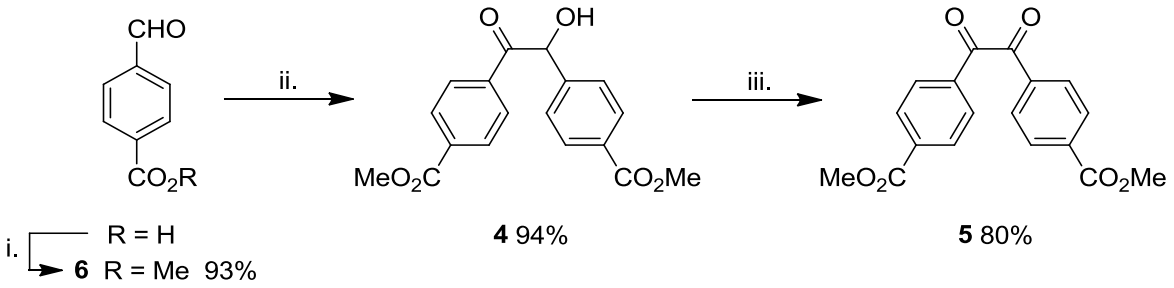

Scheme 2.4: i. CH_3OH, H_2SO_4, reflux; ii. EtOH, KCN, H_2O, 40 °C; iii. 48% HBr, DMSO, 55 °C.

The synthesis of **6** was sometimes accompanied by the formation of the corresponding acetal, **7**, identified in varying percentages (the reaction was performed several times) in the ^{1}H NMR spectrum of the material obtained upon work-up of the esterification reaction. The key signals associated with **7** were the additional singlets at δ 3.31 ppm from the acetal OMe groups and the acetal CH proton at δ 5.42 ppm (Figure 2.3).

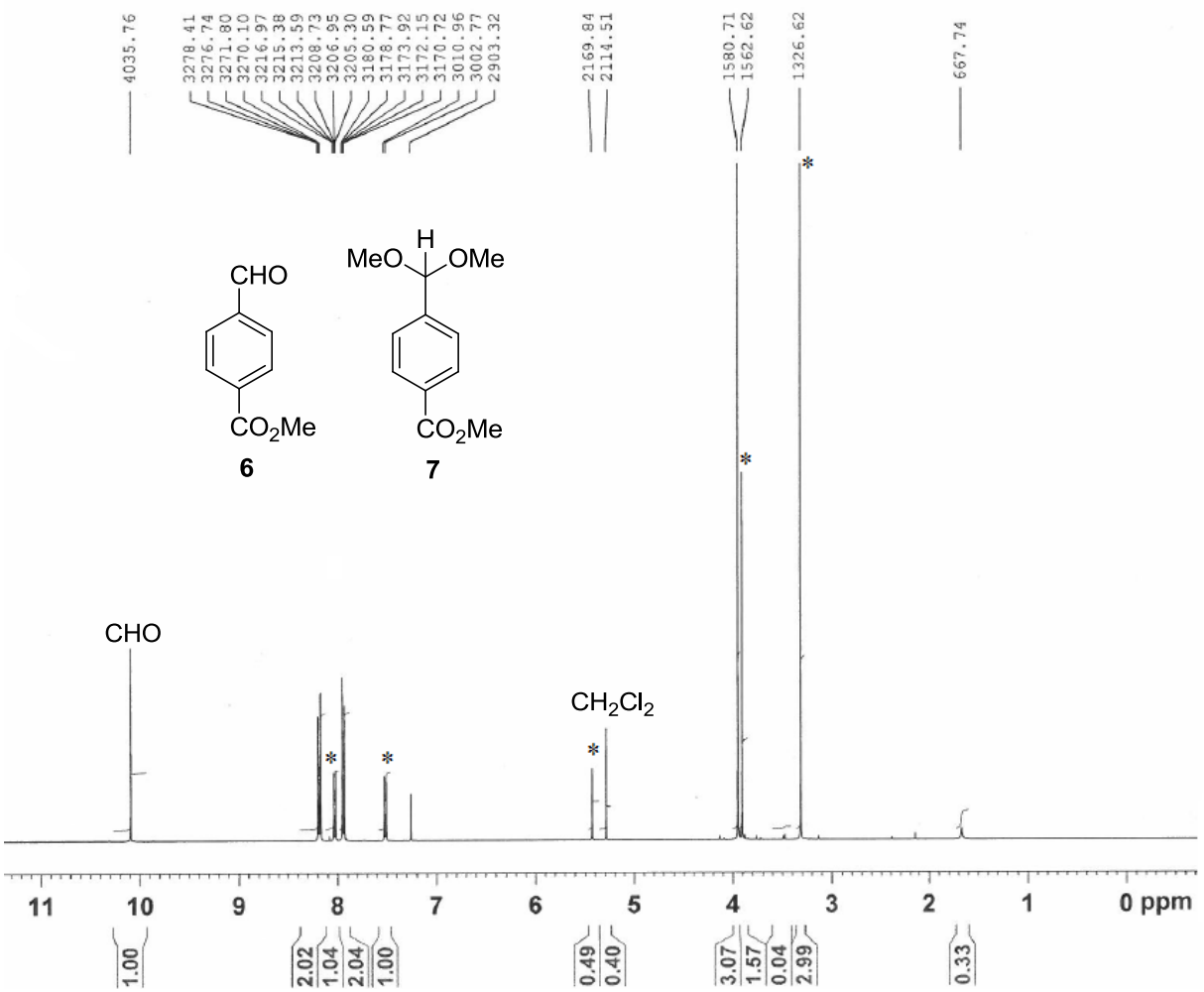

Figure 2.3: 400 MHz ^{1}H NMR spectrum ($CDCl_3$, 298 K) of a 2:1 mixture of **6** and **7** obtained after work-up (prior to overnight stirring in 1 M hydrochloric acid solution). The signals attributed to **7** are indicated with an asterisk (*).

The acetal was readily converted to the desired aldehyde by stirring the mixture of **6** and **7** in 1 M hydrochloric acid at room temperature overnight.

Substituted benzil **5** was then separately reacted with three different 1,2-diaminobenzenes, using the same chemistry as outlined in Scheme 2.2 to afford quinoxalines **8** – **10** (Scheme 2.5).

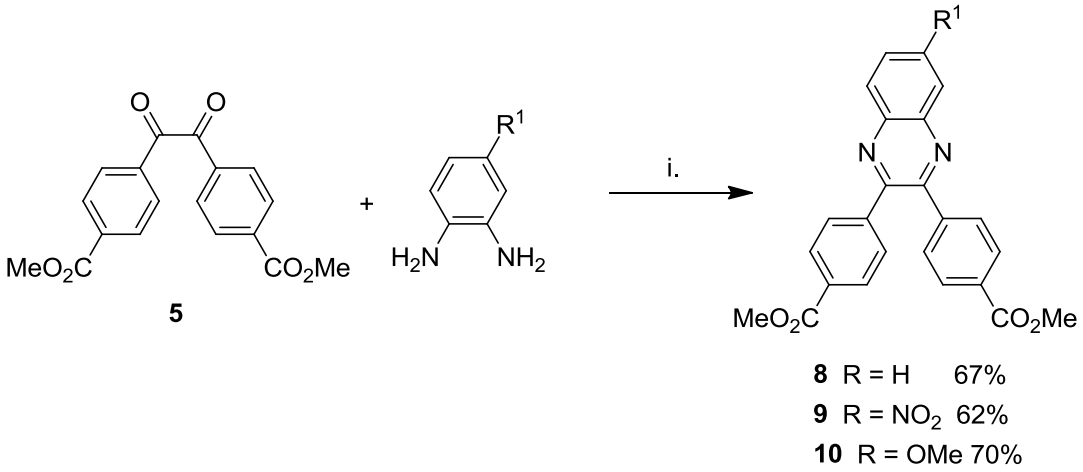

Scheme 2.5: i. glacial acetic acid, reflux.

1,2-Diamino-4-methoxybenzene **11** (used in the synthesis of **10**) was prepared in near quantitative yield by hydrogenation of 2-nitro-4-methoxyaniline (Scheme 2.6).

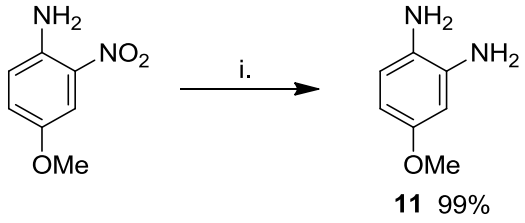

Scheme 2.6: i. H_2, EtOH, Pd/C.

Quinoxaline **8** was then reacted with 4-bromoacetophenone, with the aim of making a bis 1,3-diketone **12** (Scheme 2.7) ligand for both boron chelation and the formation of lanthanide ion complexes.

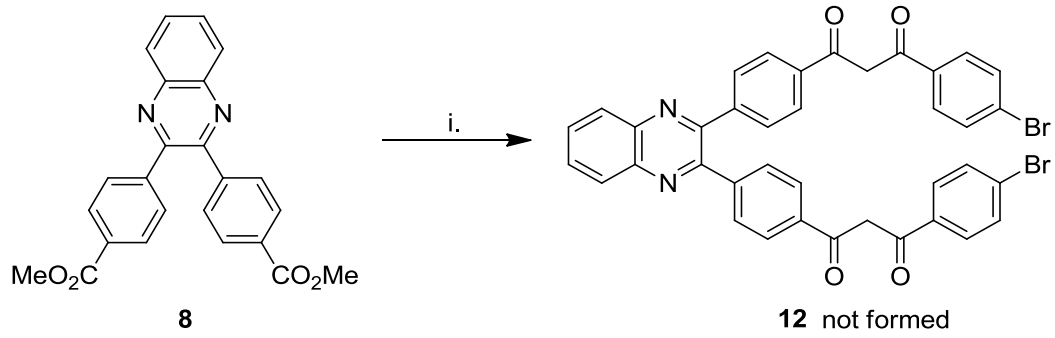

Scheme 2.7: i. 4-bromoacetophenone, NaOMe, THF, Ar atm., reflux, overnight.

Unfortunately, **12** was not obtained, but a mixture of unconverted **8**, 4-bromoacteophenone, and the 2,3-di(4'-carboxyphenyl)quinoxaline (*via* ester hydrolysis of **8**) was evident following TLC analysis of the mixture after work-up and ^{1}H NMR of the crude material. The formation of the ester hydrolysis product is the result of "wet" tetrahydrofuran. This is currently an

ongoing issue in the Department, as a decision was made over 12 months ago to remove all solvent stills, and the commercially available solvent supplied by the Department is not sufficiently anhydrous. Up until removal of the solvent stills other group members were routinely preparing 1,3-diketones in this manner in yields of 50-80% from freshly distilled tetrahydrofuran, but none have been successful with the solvent supplied in its place.

A submission will be made to the Department to allow the reintroduction of the tetrahydrofuran still and it is expected that this reaction will be successful. 4-Bromoacetophenone was chosen in the above reaction as the presence of the heavy atoms (bromo groups) would aid in solving the X-ray crystal structure, if suitable crystals can be grown. Additionally, the bromo groups provide a point for further tuning of the photophysical properties of the compound *via*, for example, Suzuki coupling reactions. Finally, the anticipated product should have a relatively simple ^{1}H NMR spectrum to analyse.

2.3 Synthesis of Precursors to Methylene-Linked Quinoxaline Ligands

A ligand in which each of the aryl rings are connected to the quinoxaline ring at the 2- and 3-positions *via* a methylene group, rather than the direct aryl-aryl linkages in the target compound shown in Figure 2.1, would serve as an analogue of the recently reported methylene linked analogue of BHHCT, BHHBCB (see Section 1.6, Figure 1.11).[19c]

It was planned to prepare quinoxaline analogues of BHHBCB using the same strategy employed in making BHHBCB. This route first required the availability of compounds of the type **13** and **14**, which could be prepared from the condensation of 1,4-dibromo-2,3-butanedione with an appropriate 1,2-diaminobenzene, as shown in Scheme 2.8 (for just two compounds at this stage).

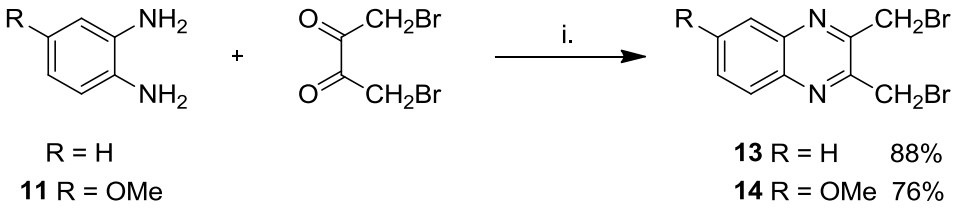

Scheme 2.8: i. EtOH.

Compound **13** was then subjected to the same reaction conditions (Scheme 2.9) as used on α,α'-dibromomethyl-*o*-xylene in the synthesis of BHHBCB,[19c] however there was no evidence of the desired product **15** following analysis of the ^{1}H NMR spectrum of the crude material after work-up. TLC analysis of the crude material after work up showed that the

quinoxaline starting material was not present, and this was also confirmed in the ^{1}H NMR spectrum. The ^{1}H NMR spectrum lacked any significant signals in the benzylic region (δ 4-6 ppm, depending upon whether the methylenes are bromobenzylic or doubly benzylic), and at this stage the major product of the reaction is unknown. The catalyst used here is unusual for a Suzuki reaction as palladium(0) is generally employed.

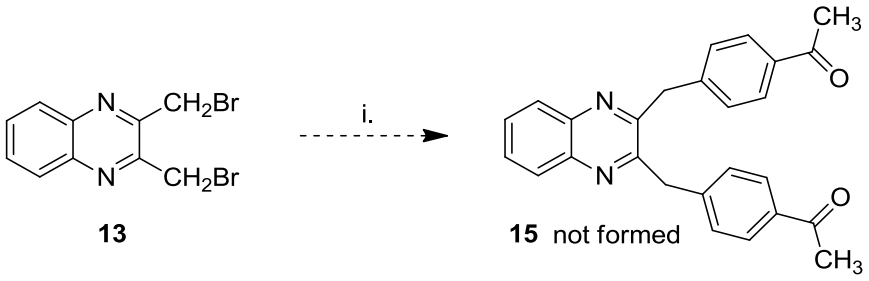

13 **15** not formed

Scheme 2.9: i. 4-acetyl phenylboronic acid, $PdCl_2$, K_2CO_3, water, acetone.

In the future **13** will be screened with a range of different conditions and catalysts using an X-cube, (a flow reactor, with different catalysts available in pre-loaded cartridges that the reaction mixture is passed through) and when the appropriate conditions are found, the substituted analogue **14** and others will be used.

When compounds of the type **15** are obtained, they will be reacted with various methyl esters under basic conditions to afford bis-1,3-diketones that will be investigated as ligands for the chelation of lanthanide ions to form new long-lived fluorescent complexes, and also for their ability to form bis boron-difluoride complexes upon reaction with boron trifluoride.

2.4 Synthesis of Hydroxychalcones

The next aspect of synthetic work was also directed at preparing new fluorescent boron and lanthanide complexes. In the first part of this work, bishydroxychalcone **16** was prepared following the published procedure, as outlined in Scheme 2.10.[22]

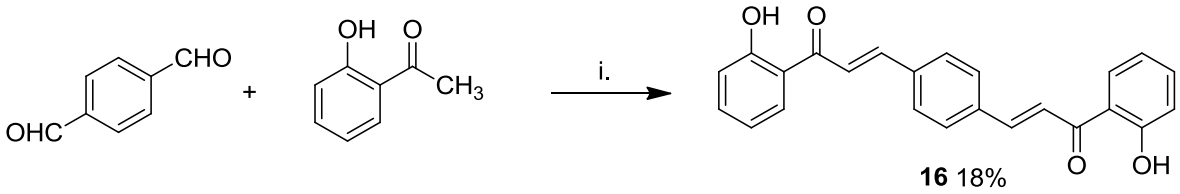

16 18%

Scheme 2.10: i. 60% NaOH in H_2O, CH_3OH, r.t., 20 h.

The double bond *E* stereochemistry was confirmed by the presence of the signals at δ 7.72 and 7.93 ppm for the four alkene protons (2H at each signal) with a 15.5 Hz coupling

constant. The symmetric nature of the compound was evident as the four protons on the central phenyl ring appeared as a singlet.

Following the successful preparation of bischalcone **16**, it was decided to take **8** and reduce it to the diol **17** and then oxidise **17** to dialdehyde **18**, as shown in Scheme 2.11.

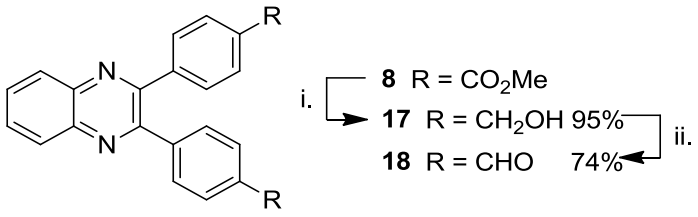

Scheme 2.11: i. $LiAlH_4$, THF, Ar atm. 0 °C to r.t. overnight; ii. MnO_2, CH_2Cl_2, 0 °C to r.t. 48 h.

The next reactions to be conducted in this part of the research will be the formation of a bis boron complex from **16** (this has not been previously reported). Dial **18** will be reacted with two equivalents of 2-hydroxyacetophenone (Scheme 2.12), under the same reaction conditions as used in Scheme 2.10 with terephthalaldehyde. Note that **19** is expected to behave as a tetradentate bis-anionic ligand in lanthanide ion chelation.

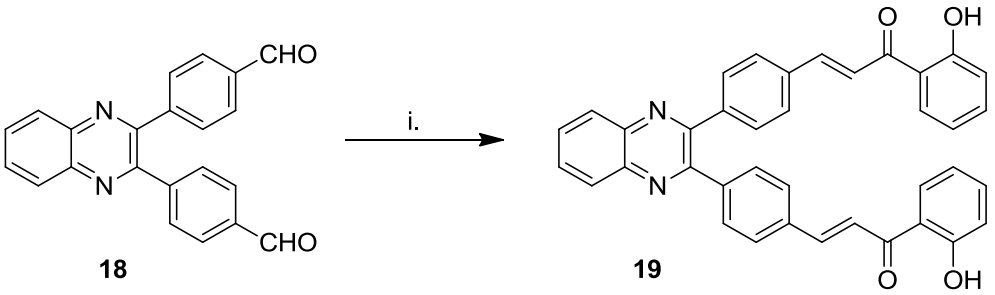

Scheme 2.12: i. 60% NaOH in H_2O, CH_3OH, r.t., 20 h.

Compound **19** will then be investigated for its ability to form complexes with lanthanide ions, and if this occurs, the photophysical properties of it, and analogues, will be studied.

2.5 Bioconjugate Synthesis and Labeling Studies

In the final component of this work, a novel protein construct, linker protein G (LPG),[23] was labeled with commercially available NHS-activated Alexa Fluor 488 (Figure 1.5). LPG is a recombinant protein version of protein G (PG). It contains a modified amino acid repeat sequence that shows an affinity for silica binding. The repeat sequence contains lysine residues, among others. The goal of this aspect of research is to bind fluorophores to the linker portion of LPG, a site remote from the binding site of LPG to its antibody partners (the

same as those of protein G). Fluorophores possessing groups capable of binding to the amino groups present on the side chains of the lysine residues in the "linker" portion of LPG are expected to become covalently bound, forming a protein-dye conjugate. Such conjugates would be analogous to commercially available protein G-dye conjugates, but as LPG contains more lysine residues, it is hoped that the LPG-dye conjugates will be much brighter, as they will have more dye molecules bound to each protein molecule. This is shown schematically in Figure 2.4A.

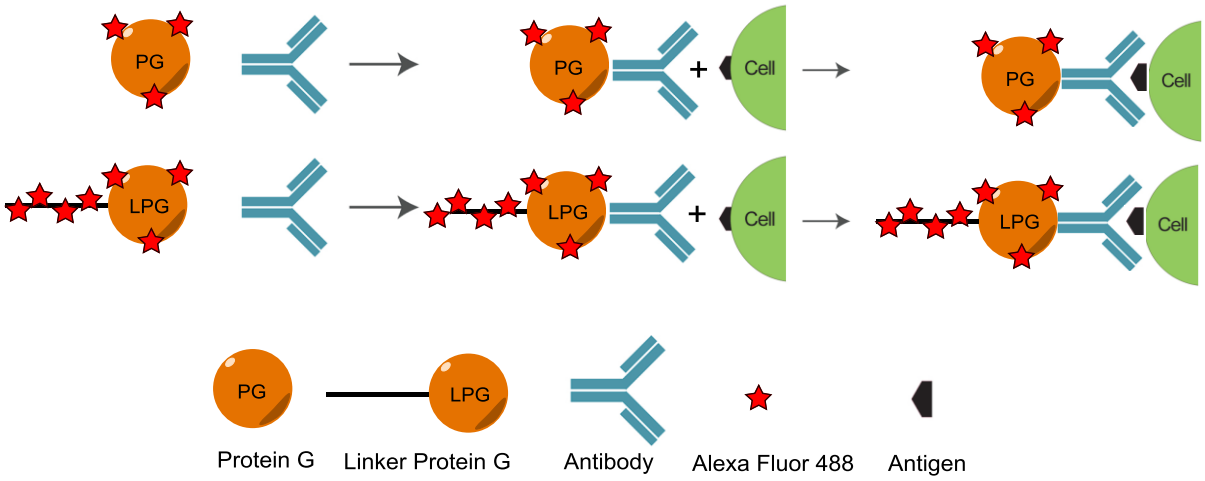

Figure 2.4A: Schematic illustration of labelling PG and LPG and the way in which they interact with an antibody, and how the assembly can label a cell.

LPG was expressed and purified as described in Section 3.7. The procedure afforded LPG in high purity, as shown in Figure 3.1. In order to make a direct comparison of the behaviour of LPG and PG, conjugation experiments were conducted with both proteins, as described in Section 3.8. Data collected on the products of the conjugation experiments (Section 3.8.4) suggested that Alexa Fluor 488 was attached to both LPG and PG (Figure 3.2 and Figure 3.3, respectively). The synthesized LPG-488 and PG-488 conjugates were found to have a dye:protein ratio of 4.7:1 and 1.4:1, respectively (Section 3.8.5). Further, to validate the PG-488 conjugate behavior, a commercial PG-488 conjugate was purchased and used in the labeling studies described below.

Cryptosporidium oocysts cells were used for imaging experiments and the antibody used for labeling of cells was the CRY104 specific antibody. The concentration of the antibody was known and from this the mole ratio of protein to antibody was calculated and used for the imaging experiments. The procedure involved the addition of a measured aliquot of 1 µL of commercial PG-Alexa Fluor 488 conjugate (6.4 pmol) to 1 µL of crypto antibody (CRY104

7.65 pmol) and dilution of the resultant solution to 10 µL with 0.1X PBS, that was then vortexed well. The mixture of protein conjugate and the antibody was then loaded onto a microscope slide, previously fixed with *Cryptosporidium oocysts* cells and incubated for 1 min at room temperature. The images were captured with an Olympus DP72 camera using a fixed exposure and camera speed of 1s and 200 ASA respectively. This ratio of protein conjugate to the antibody showed some background noise and some non-specific binding, which can be optimized in future experiments by adjusting the suitable molar ratio of protein conjugate to the antibody. The images of the cells labeled using the commercial PG-488 conjugate with CRY104 antibody are shown in Figure 2.4B.

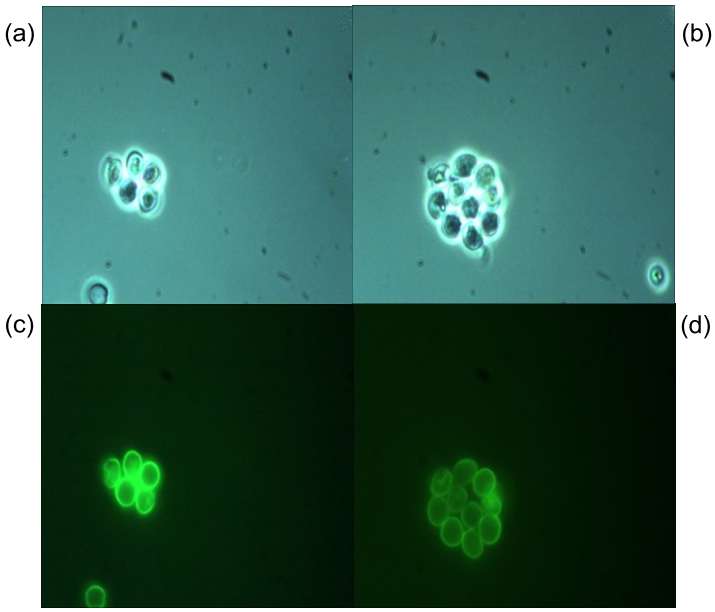

Figure 2.4B: Images of *Cryptosporidium oocysts* cells labeled with CRY104 antibody with the commercial PG labeled with Alexa 488 (PG-488). The top portion of images (a) and (b) shows the bright field image of the cells and below (c) and (d) are the corresponding cells labeled with protein G Alexa 488 conjugate.

The same method of cell labeling was followed for the prepared protein-G and LPG conjugates with the same mole ratio (approx. 1:1) and the cells were imaged under the microscope. In both cases the initial concentration used was in the pmol levels and no prominent labeling of the cells was observed. Hence the mole ratios were altered and increased slightly to 5 pmol from 1 pmol and viewed under the microscope. In this case, the images revealed no binding and showed a flood load of green background. After a series of experimental trials with the prepared PG and LPG conjugates, no labeling of cells was observed. At this stage the reason for the failure of the prepared conjugates to label the cells

is unknown, as earlier tests indicate that over-labeling with dye should not be a problem (see Section 3.8.5) and the purification steps (specifically passage through the Sephadex G-25 column) should have removed any un-conjugated Alex 488 (Section 3.8.4). According to the literature,[24] various other factors like pH of the buffer, temperature, purity of the buffer, and purity of the protein need to be checked, as slight variations in these factors might also affect labeling experiments.

Clearly all of the protocols adopted in this preliminary work need to be reviewed as part of a future study.

At the time of writing, a comparison on the use of LPG versus PG in terms of intensity of fluorescence labeling cannot be made.

A preliminary experiment as described in Section 3.9 was performed with the assistance of Dr. Anwar Sunna, so as to further probe the unsuccessful labeling of the prepared PG and LPG conjugates.

Dynabeads (from Life Technologies) with Goat anti-Mouse IgG in combination with primary mouse IgG antibodies were used in a binding experiment and it was observed that the LPG-488 and synthesized PG-488 conjugates had no binding towards the antibody, thus leading to flood load of green background and non-specific binding when viewed under the microscope. As a control experiment, the commercial PG-488 conjugate was used in the same experimental set-up to confirm that the Dynabeads were behaving as expected, and in this instance green fluorescence was associated with the beads when viewed under the microscope, confirming an interaction between the beads and the commercially labelled PG.

This result establishes that the failure to label the cells has its origins in the conjugate-antibody interaction, rather than the (conjugate-antibody)-cell interaction.

2.6 Summary

Two routes to a quinoxaline analogue of BHHCT were investigated. A strategy involving the preparation of a bis-4'-acetyl-2,3-diphenylquinoxaline was unsuccessful, however bis 4'-methyl esters **8**-**10** were prepared in good yields. These compounds need to be converted to bis 1,3-diketones *via* reaction with suitable methyl ketones to afford the desired ligand frameworks, in which the central phenyl ring of BHHCT is replaced with a quinoxaline ring. This work requires the use of dry solvents that should be available in the very near future. The ability of the targeted ligands to sensitize Eu^{3+} and Tb^{3+} will then be investigated.

Work was commenced on the syntheses of quinoxaline-based analogues of BHHBCB. A suitable catalyst needs to be found for the Suzuki coupling reaction.

Bis methyl ester **8** was converted to dial **18**. This compound will be converted to bis chalcone **19**, that is expected to chelate Eu^{3+} ions as the 2-hydroxyphenyl ketone portion of the molecule is iso-structural with the enol tautomer of 1,3-diketones.

LPG was successfully expressed and purified. The dye Alexa Fluor 488 was conjugated to both LPG and PG. A commercial PG-488 conjugate was use to successfully label *Cryptosporidium oocysts* cells, however the synthetic conjugates in their current state were shown to be incapable of interacting with the PG antibody. Further work needs to be done to more comprehensively characterize the synthetic LPG-488 and PG-488 conjugates, including HPLC analysis and varying the pH of the current material.

Chapter Three Experimental

3.1 General Procedures

^{1}H NMR spectra were recorded on a Bruker WM AMX 400 spectrometer (400 MHz) at 300 K unless otherwise stated. Signals were recorded in terms of chemical shifts, multiplicity, coupling constants (in Hz). The following abbreviations for multiplicity are used: s, singlet; d, doublet; t, triplet; m, multiplet, dd, doublet of doublets, app, apparent, meaning has the appearance of a given multiplicity, but is actually more complex. Solvents and reagents were purified using standard techniques. All commercial solvents were HPLC grade. Where solvent mixtures are used, the portions are given by volume.

Column chromatography was routinely carried out using the gravity feed column techniques on Merck silica gel type 9385 (230-400 mesh) with the stated solvent systems. Analytical thin layer chromatography (TLC) analyses were performed on Merck silica gel 60 F254 protected sheets (0.2 mm). Visualisation of compounds was achieved by illumination under ultraviolet light (254 nm).

Protein G was purchased from Sigma Aldrich, Alexa Fluor 488-NHS ester and Protein G-Alexa Fluor 488 conjugate were purchased from Life Technologies Australia.

3.2 Preparation of Quinoxalines from Benzil

3.2.1 General Preparation of Quinoxalines

The benzil (1.0 mmol) was dissolved in glacial acetic acid (7 mL) and to this was added a solution of the 1,2-diaminobezene (2.1 eq.) in glacial acetic acid (4 mL). The resultant solution was stirred and heated at reflux for 48 h under an argon atmosphere. The reaction mixture was then cooled to room temperature and evaporated to dryness. The residue was taken up in a mixture of dichloromethane and water (1:1 by volume). Sodium carbonate was added in small portions until the acidic solution was neutralised. The organic phase was then separated and the aqueous phase was further extracted with dichloromethane. The combined organic layers were washed with saturated sodium bicarbonate solution, water and brine. The organic layer was dried over magnesium sulfate, filtered and evaporated to dryness to afford crude material.

3.2.2 2,3-Diphenylquinoxaline 1

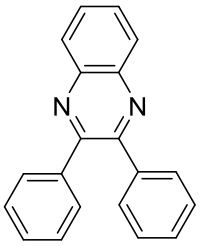

Using benzil (2.00 g, 9.75 mmol) and *ortho*-phenylenediamine (2.25 g, 20.80 mmol, 2.1 eq.), the crude material was chromatographed (silica; ethyl acetate:hexane, 20:80) to afford 2,3-diphenylquinoxaline **1** (2.60 g, 96%) as a pale yellow powder. m.p. 127-129 °C (lit.[25] 126-127 °C); ^{1}H NMR (400 MHz, $CDCl_3$) δ 7.31-7.40 (6H, m, ArH), 7.50-7.56 (4H, m, ArH), 7.75-7.81 (2H, m, quinoxaline H), 8.16-8.23 (2H, m, quinoxaline H). The data is in agreement with those reported in the literature.[25]

3.2.3 6-Nitro-2,3-diphenylquinoxaline 2

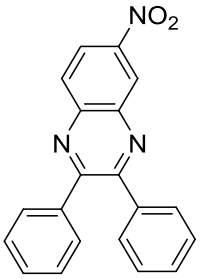

Using benzil (2.00 g, 9.75 mmol) and 4-nitro-1,2-diaminobenzene (2.18 g, 14.20 mmol), the crude material was chromatographed (silica; dichloromethane:hexane, 25:75) to afford 6-nitro-2,3-diphenylquinoxaline **2** (1.99 g, 64%) as a pale yellow powder. m.p. 189-190 °C (lit.[25] 192-193 °C); ^{1}H NMR (400 MHz, $CDCl_3$) δ 7.33-7.46 (6H, m, ArH), 7.52-7.60 (4H, m, ArH), 8.30 (1H, d J = 9.1 Hz, quinoxaline H), 8.53 (1H, dd J = 2.5 9.1 Hz, quinoxaline H), 9.08 (1H, d J = 2.5 Hz, quinoxaline H). The data is in agreement with those reported in the literature.[25]

3.3 Acetylation Reactions

3.3.1 Diacetyl-*o*-terphenyl (a model reaction)

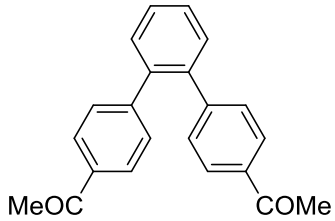

Ortho-terphenyl (1.00 g, 4.30 mmol) was dissolved in dry dichloromethane (5 mL) in a closed container under an argon atmosphere. In another round bottom flask, under a nitrogen atmosphere, aluminium chloride (1.30 g, 9.75 mmol, 2.25 eq.) was dissolved in dry dichloromethane (20 mL) and acetyl chloride (0.84 g, 10.70 mmol, 2.5 eq.) was added, with stirring. This mixture was maintained at 0 °C and was added to the *ortho*-terphenyl solution in drop-wise manner. A violet coloured solution was observed upon addition of the acetylation reagents. The mixture was stirred for another 1 h at 0 °C and kept in room temperature overnight with continuous stirring. The reaction mixture was then heated at reflux for 4 h, resulting in the formation of a dark brown mixture that was allowed to cool to room temperature. The reaction mixture was then added to a separatory funnel containing ice (250 g) and hydrochloric acid (3 M, 20 mL). The aqueous layer was extracted with dichloromethane (2 x 50 mL) and the combined organic layers were washed with brine (100 mL), dried over magnesium sulfate, filtered and evaporated to dryness. The crude material was then chromatographed (silica; ethyl acetate:hexane, 20:80) to afford diacetyl-*o*-terphenyl **3** (1.12 g, 83%) as a pale white powder. m.p. 174-177 °C; ^{1}H NMR (400 MHz, $CDCl_3$) δ 2.57 (6H, s, CH_3), 7.22 (4H, app. d, J = 8.3 Hz, ArH), 7.41 – 7.51 (4H, m, ArH), 7.82 (4H, app. d, J = 8.3 Hz, ArH). The data is in agreement with those reported in the literature.[18a]

3.3.2 Attempted Preparation of 2,3-Bis-(4'-acetylphenyl)quinoxaline

As for the synthesis of **3**, using 2,3-diphenylquinoxaline **1** (1.00 g, 3.49 mmol), aluminium chloride (1.05 g, 7.90 mmol, 2.25 eq.) and acetyl chloride (685 mg, 8.70 mmol, 2.5 eq.) with stirring. Upon addition of the acetylation reagents a cherry red coloured solution resulted. Immediately prior to work-up, the reaction mixture appeared as a dark brown liquid that after work-up afforded a pale yellow powder (965 mg). The crude sample was then analysed over thin layer chromatography indicating that unconverted **1** was recovered in essentially pure form. This was confirmed by ^{1}H NMR analysis.

3.3.3 Attempted Preparation of 2,3-Bis-(4'-acetylphenyl)-6-nitroquinoxaline

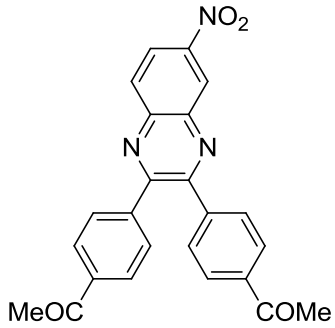

As for the synthesis of **3**, using 6-nitro-2,3-diphenylquinoxaline **2** (1.00 g, 3.05 mmol), aluminium chloride (0.91 g, 6.90 mmol, 2.26 eq.) and acetyl chloride (0.60 g, 7.60 mmol, 2.5 eq.). Upon addition of the acetylation reagents a pale yellow colour solution resulted. Immediately prior to work-up, the reaction mixture appeared as a dark brown liquid that after work-up afforded a pale yellow powder (950 mg). The crude sample was then analysed over thin layer chromatography indicating that unconverted **2** was recovered in essentially pure form. This was confirmed by ^{1}H NMR analysis.

3.4 Preparation of Dimethyl Ester Substituted Quinoxalines

3.4.1 1,2-Diamino-4-methoxybenzene 11

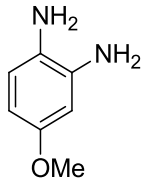

4-Methoxy-2-nitroaniline (1.00 g, 5.9 mmol) was dissolved in a mixture of ethanol (50 mL) and dichloromethane (15 mL). Palladium on carbon (10%, 100 mg) was added and the reaction mixture was stirred under an atmosphere of hydrogen overnight. The mixture was then filtered through celite and evaporated to dryness under vacuum to afford 1,2-diamino-4-methoxybenzene **11** (820 mg, 99%) as a dark violet sticky solid that was used without further purification; ^{1}H NMR (400 MHz, $CDCl_3$) δ 2.70 (4H, s, NH_2), 3.73 (3H, s, OCH_3), 6.26 (1H, dd, J = 2.5, 8.4 Hz, ArH), 6.32 (1H, d, J = 2.5 Hz, ArH), 6.65 (1H, d, J = 8.4 Hz, ArH).

3.4.2 Methyl-4-formylbenzoate 6

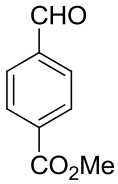

4-Formylbenzoic acid (10.00 g, 66.60 mmol) dissolved in methanol (100 mL), followed by the addition of sulfuric acid (18 M, 4 mL). The reaction mixture was heated at reflux for 48 h. The reaction mixture was then cooled to room temperature and evaporated to dryness. The residue was dissolved in a mixture of dichloromethane (50 mL) and water (50 mL), followed by addition of sodium carbonate in small portions to neutralise the sulfuric acid. The organic phase was then separated and the aqueous phase was further extracted with dichloromethane (2 x 50 mL). The organic layers were combined and washed with saturated sodium bicarbonate (100 mL), water (50 mL) and brine (100 mL). The organic layer was dried over magnesium sulfate, filtered and evaporated to dryness. The crude material was chromatographed (silica; dichloromethane) to afford methyl-4-formylbenzoate **6** (10.18 g, 93%) as a white shiny powder. m.p. 62-64 °C (lit.[26] 61-62 °C); ^{1}H NMR (400 MHz, $CDCl_3$) δ 4.00 (3H, s, CH_3), 7.96 (2H, app. d, J = 8.2 Hz, ArH), 8.19 (2H, app. d, J = 8.2 Hz, ArH), 10.09 (1H, s, CHO). The data is in agreement with those reported in the literature.[26]

3.4.3 4,4'-Dimethylcarbonylbenzoin 4

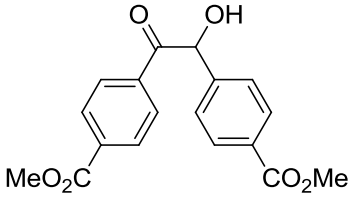

Methyl-4-formylbenzoate **6** (5.00 g, 30.5 mmol) was dissolved in ethanol (100%, 35 mL) with continuous stirring. Potassium cyanide (0.60 g, 9.20 mmol) was added to the reaction mixture, followed by the addition of water (20 mL). The reaction mixture was then heated at 40 °C for 75 mins. The reaction mixture was then cooled to room temperature, filtered and washed with water to remove cyanide and dried, yielding 4,4'-dimethylcarbonylbenzoin **4** (4.64 g, 94%) as a pale brown powder that was used without further purification. m.p. 138-139 °C (lit.[20] 140-141 °C); ^{1}H NMR (400 MHz, $CDCl_3$) δ 3.87 (3H, s, CH_3), 3.91 (3H, s, CH_3), 4.52 (1H, d, J = 5.2 Hz, OH), 6.01 (1H, d, J = 5.2 Hz, CH), 7.40 (2H, d, J = 8.2 Hz, ArH), 7.92 (2H, d, J = 8.3 Hz, ArH), 7.98 (2H, d, J = 8.2 Hz, ArH), 8.05 (2H, d, J = 8.3 Hz, ArH). The data are in agreement with those reported in the literature.[20]

3.4.4 4,4'-Dimethylcarbonylbenzil 5

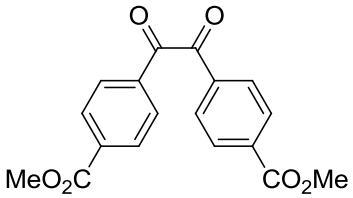

4,4'-Dimethylcarbonylbenzoin **4** (4.00 g, 12.2 mmol) was dissolved in DMSO (30 mL) and with continuous stirring hydrobromic acid (48%, 6 mL) was added slowly. The reaction mixture was heated at 55 °C in oil bath and allowed to continue for 24 h. The reaction mixture was then cooled to room temperature, filtered and washed with water to remove DMSO. The crude material was then dried under vacuum to afford 4,4'-dimethylcarbonylbenzil **5** (3.00 g, 80%) as a bright yellow powder that was used without further purification. m.p. 197-198 °C (lit.[20] 197-198 °C); ^{1}H NMR (400 MHz, $CDCl_3$) δ 3.97 (6H, s, CH_3), 8.05 (4H, app. d, J = 8.5 Hz, ArH), 8.18 (4H, app. d, J = 8.5 Hz, ArH). The data are in agreement with those reported in the literature.[21]

3.4.5 2,3-Di(4'-methoxycarbonylphenyl)quinoxaline 8

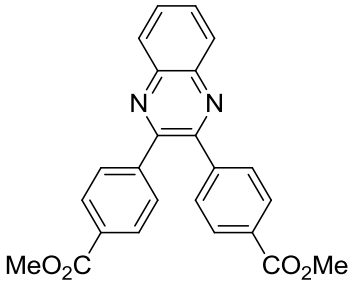

4,4'-Dimethylcarbonylbenzil **5** (1.00 g, 3.1 mmol) and *o*-phenylenediamine (0.75 g, 6.9 mmol) were dissolved in glacial acetic acid (50 mL) and the reaction mixture was stirred and refluxed under an argon atmosphere for 48 h. The reaction mixture was then cooled to room temperature and the evaporated to dryness to remove the excess acetic acid. The residue was dissolved in a mixture of dichloromethane (50 mL) and water (50 mL). Sodium carbonate was added in small portions until the acidic solution was neutralised. The organic phase was then separated and the aqueous phase was further extracted with dichloromethane (2 x 50 mL). The organic layers were combined and washed with saturated sodium bicarbonate (100 mL), water (50 mL) and the brine (100 mL). The organic layer was then dried over magnesium sulfate, filtered and evaporated to dryness. The crude sample was then chromatographed (silica; ethyl acetate:hexane, 2:8) to afford 2,3-di(4'-methoxycarbonylphenyl)quinoxaline **8** (0.80 g, 67%) as a white powder. m.p. 232-233 °C

(lit. [27] 239-240 °C); ^{1}H NMR (400 MHz, $CDCl_3$) δ 3.94 (6H, s, CH_3), 7.58 (4H, app. d, *J* = 8.5 Hz, ArH), 7.82 – 7.86 (2H, m, quinoxaline H), 8.01 (4H, app. d, *J* = 8.5 Hz, ArH), 8.18 – 8.23 (2H, m, quinoxaline H); ^{13}C NMR (100 MHz, $CDCl_3$) δ 52.27, 129.29, 129.63, 129.91, 130.47, 130.72, 141.28, 142.96, 152.19, 166.57. There are no reported NMR data for this compound, just m.p. and elemental analysis data.[27]

3.4.6 2,3-Di(4'-methoxycarbonylphenyl)-6-nitroquinoxaline 9

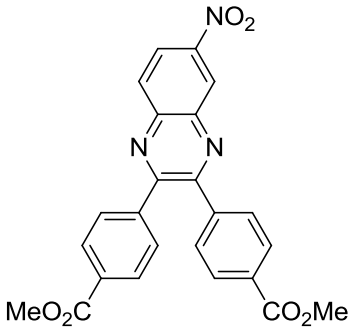

Was synthesised as described for the preparation of **8**, using 4,4'-dimethylcarbonylbenzil **5** (1.00 g, 3.1 mmol) and 4-nitrobenzene-1,2-diamine (1.05 g, 6.8 mmol, 2.25 eq.). The crude material was then chromatographed (silica; methanol:dichloromethane, 2:98) to afford 2,3-di(4'-methoxycarbonylphenyl)-6-nitroquinoxaline **9** (830 mg, 62%) as a brown powder. m.p. 201-203 °C; ^{1}H NMR (400 MHz, $CDCl_3$) δ 3.94 (6H, s, CH_3), 7.58-7.66 (4H, m, ArH), 8.04 (4H, d, *J* = 8.3 Hz, ArH), 8.33 (1H, d, *J* = 9.2 Hz, ArH), 8.58 (1H, dd, *J* = 9.2 Hz, 2.5 Hz, ArH), 9.10 (1H, d, *J* = 2.5 Hz, ArH). ^{13}C NMR (100 MHz, $CDCl_3$) δ 52.38, 123.94, 125.71, 129.76, 129.89, 129.95, 130.96, 131.19, 131.28, 140.09, 141.83, 141.90, 143.53, 148.29, 154.46, 155.07, 166.34, 166.36.

3.4.7 2,3-Di(4'-methoxycarbonylphenyl)-6-methoxyquinoxaline 10

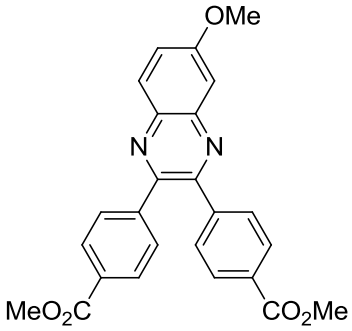

Was synthesised as described for the preparation of **8**, using 4,4'-dimethylcarbonylbenzil **5** (950 mg, 2.9 mmol) and 4-methoxybenzene-1,2-diamine **11** (830 mg, 6.5 mmol, 2.25 eq.). The crude material was then chromatographed (silica; methanol:dichloromethane, 4:96) to afford 2,3-di(4'-methoxycarbonylphenyl)-6-methoxyquinoxaline **10** (840 mg, 70%) as a

brown powder. m.p. 154-155 °C; ^{1}H NMR (400 MHz, $CDCl_3$) δ 3.92 (3H, s, CO_2CH_3), 3.93 (3H, s, CO_2CH_3), 4.01 (3H, s, OCH_3), 7.48 (1H, dd, *J* = 2.7, 9.2 Hz quinoxaline H), 7.53 (1H, d, *J* = 2.7 Hz, quinoxaline H), 7.54 – 7.9 (4H, m, ArH), 7.96 – 8.05 (4H, m, ArH), 8.09 (1H, d, *J* = 9.2 Hz, quinoxaline H). ^{13}C NMR (100 MHz, $CDCl_3$) δ 52.23, 52.25, 56.00, 106.06, 124.51, 129.60, 129.64, 129.88, 129.92, 130.21, 130.24, 130.49, 137.64, 142.56, 142.74, 142.92, 149.54, 151.78, 161.65, 166.56, 166.61.

3.5 Toward Preparation of Quinoxaline Analogues of BHHBCB

3.5.1 2,3-Bis(bromomethyl)quinoxaline 13

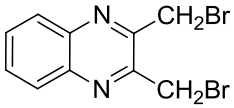

1,4-Dibromo-2,3-butanedione (2.00 g, 8.16 mmol) was dissolved in ethanol (50 mL) with continuous stirring and cooled to 0 °C. *o*-Phenylenediame (1.16 g, 8.36 mmol) was also dissolved in ethanol (10 mL) and cooled to 0 °C. Both solutions were mixed together and maintained at 0 °C for 2 h and then stirred at room temperature overnight. The reaction mixture was evaporated to dryness and the crude material was chromatographed (silica; dichloromethane) yielding 2,3-bis(bromomethyl)quinoxaline **13** (2.26 g, 88%) as a pale brown powder. ^{1}H NMR (400 MHz, $CDCl_3$) δ 4.96 (4H, s, CH_2), 7.81-7.86 (2H, m, quinoxaline H), 8.11-8.16 (2H, m, quinoxaline H).

3.5.2 2,3-Bis(bromomethyl)-6-methoxyquinoxaline 14

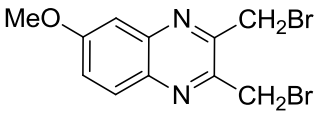

1,4-Dibromo-2,3-butanedione (1.47 g, 6.0 mmol) was dissolved in ethanol (75 mL) with continuous stirring and cooled to 0 °C. 1,2-Diamino-6-methoxybenzene **11** (850 mg, 6.15 mmol) was also dissolved in ethanol (10 mL) and cooled to 0 °C. Both solutions were mixed together and maintained at 0 °C for 2 h and then stirred at room temperature overnight. The reaction mixture was evaporated to dryness and the crude material was chromatographed (silica; dichloromethane) yielding 2,3-bis(bromomethyl)-6-methoxyquinoxaline **14** (1.58 g, 76%) as a pale brown powder. m.p. 129-131 °C (lit.[28] 133-134 °C); ^{1}H NMR (400 MHz, $CDCl_3$) δ 3.98 (3H, s, OCH_3), 4.89 (2H, s, CH_2), 4.90 (2H, s, CH_2), 7.35 (1H, d, *J* = 2.7 Hz, quinoxaline H), 7.43 (1H, dd, *J* = 2.7, 9.2 Hz, quinoxaline H), 7.94 (1H, d, *J* = 9.2 Hz, quinoxaline H). ^{13}C NMR (100 MHz, $CDCl_3$) δ 30.33, 30.67, 55.94, 106.13, 124.57, 129.98,

137.54, 143.01, 147.97, 150.63, 160.78. The data are in agreement with those reported in the literature.[28]

3.5.3 Attempted preparation of 2,3-bisbenzylquinoxaline 15

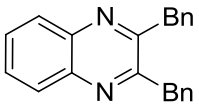

2,3-Bis(bromomethyl)quinoxaline **13** (1.00 g, 3.2 mmol) and phenylboronic acid (2.60 g, 11.4 mmol, 3.6 eq.) were dissolved in acetone (24 mL) and stirred well, and potassium carbonate (2.20 g, 16.0 mmol, 5.0 eq.) was added. Water (8 mL) was added and the mixture was heated slightly to solubilize all reactants. Palladium(II) chloride (77 mg) was added by to the ice-cooled reaction mixture ice bath with continuous stirring. After 30 minutes of stirring in ice, the reaction mixture was heated in oil bath at 50 °C under an argon atmosphere overnight. After 24 h, the reaction mixture was cooled to room temperature and evaporated to dryness. The residue was dissolved in a mixture of dichloromethane (100 mL) and water (100 mL). The organic phase was then separated and the aqueous phase was further extracted with dichloromethane (2 x 50 mL). The organic layers were combined and washed with water (50 mL) and the brine (100 mL). The organic layer was then dried over magnesium sulfate, filtered and evaporated to dryness to afford crude material (1.16 g). The crude sample was then analysed over thin layer chromatography indicating that no major product was formed.

3.6 Chalcone Chemistry as Ligands for Boron and Europium Complex Formation

3.6.1 (2*E*,2'*E*)-3,3'-(1,4-pheneylene)bis(1-(2-hydroxyphenyl)prop-2-ene-1-one) 16

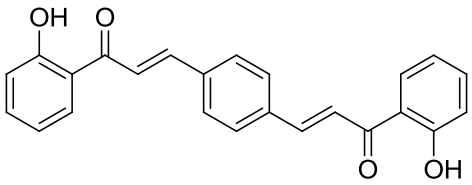

An aqueous solution of sodium hydroxide (60%, 70 mL) was added to a solution (100 mL) of 2-hydroxyacetophenone (2.04 g, 15.0 mmol, 2 eq.) in methanol (100 mL). After cooling to room temperature suspension of terephthaldehyde (1.00 g, 7.55 mmol, 1 eq.) in methanol (20 mL) was added and the resulting mixture was stirred at room temperature for 20 h. The reaction mixture was acidified to pH 2 by the addition of hydrochloric acid, filtered and washed with water. The resulting yellow solid was dissolved in dichloromethane (150 mL) and washed with saturated sodium hydrogen carbonate solution (2 x 100 mL), brine (100

mL), dried over anhydrous sodium sulfate, filtered and evaporated to dryness. The crude material was then chromatographed (silica; dichloromethane) to afford (2*E*,2'*E*)-3,3'-(1,4-pheneylene)bis(1-(2-hydroxyphenyl)prop-2-ene-1-one) **16** (840 mg, 18%) as a yellow powder. m.p. 257-259 °C (lit.[22] 259-261 °C); ^{1}H NMR (400 MHz, $CDCl_3$) δ 6.95 – 7.00 (2H, m, ArH), 7.04 – 7.07 (2H, m, ArH), 7.50 – 7.56 (2H, m, ArH), 7.72 (2H, *J* = 15.5 Hz, alkene H), 7.74 (4H s, ArH), 7.90 – 7.96 (4H, m, ArH and alkene H), 12.74 (2H, s, OH). The data is in agreement with that in the literature.[22]

3.6.2 2,3-Bis(4'-hydroxymethylphenyl)quinoxaline 17

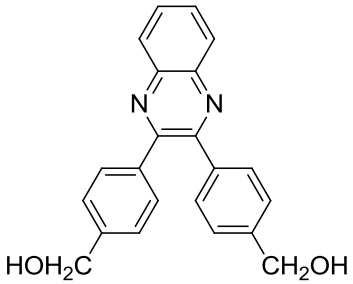

Lithium aluminium hydride (1.14 g, 30.0 mmol) was dispersed in dry THF (40 mL), and the mixture stirred under an argon atmosphere in ice flask for 30 min. 2,3-Di(4'-methoxycarbonylphenyl)quinoxaline **8** (910 mg, 2.30 mmol) was dissolved in dry THF (15 mL) and added to the mixture. The reaction mixture stirred under an argon atmosphere at 0 °C and allowed to reach room temperature overnight. Water (4 mL) and 15% sodium hydroxide solution (10 mL) were added to the reaction mixture (dropwise) respectively, and then water (10 mL) was added to provide an inorganic precipitate that was easy to rinse and filter after 2 h. The reaction mixture was filtered and rinsed with dichloromethane and extracted with dichloromethane (3 x 50 mL) and water. The organic layer was washed with brine, dried over anhydrous sodium sulfate, filtered and evaporated to dryness to afford the 2,3-bis(4'-hydroxymethylphenyl)quinoxaline **17** (750 mg, 95%) that was used without further purification. m.p. 212-214 °C; ^{1}H NMR (400 MHz, $CDCl_3$) δ 1.92 (2H, br s, OH), 4.71 (4H, s, CH_2), 7.31-7.33 (4H, app. d, *J* = 8.0 Hz, ArH), 7.51-7.53 (4H, app. d, *J* = 8.0 Hz, ArH), 7.77-7.80 (2H, m, quinoxaline H), 8.19-8.22 (2H, m, quinoxaline H); ^{13}C NMR (100 MHz, $CDCl_3$) δ 65.6, 127.8, 130.2, 131.2, 131.3, 139.2, 142.2, 143.0, 154.3.

3.6.3 2,3-Bis(4'-formylphenyl)quinoxaline 18

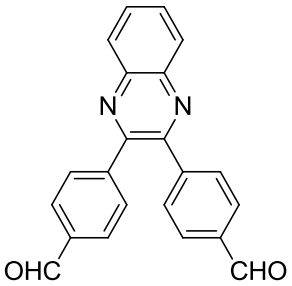

Manganese dioxide (3.56 g, 41.0 mmol) was added to a solution of **17** (700 mg, 2.05 mmol) and dichloromethane (85 mL) at 0 °C and stirred for 30 min with a drying tube attached. The reaction mixture then was allowed to warm to a room temperature and stirred overnight. The reaction was monitored by TLC and more manganese dioxide (1.78 g, 20.5 mmol) was added and stirred for another night. After completion the mixture was filtered through celite and the solvent was evaporated to dryness to afford 2,3-bis(4'-formylphenyl)quinoxaline **18** (515 mg, 74%) that was used without further purification. m.p. 165-166 °C; ^{1}H NMR (400 MHz, $CDCl_3$) δ 7.69-7.71 (4H, m, ArH), 7.83-7.89 (6H, m, 4 ArH and 2 quinoxaline H), 8.20-8.24 (2H, m, quinoxaline H), 10.10 (2H, s, CHO). ^{13}C NMR (100 MHz, $CDCl_3$) δ 129.77, 130.12, 131.00, 131.41, 136.73, 141.75, 144.73, 152.18, 192.06.

3.7 Production and Purification of Recombinant LPG

Recombinant LPG was produced in *E. coli* and purified by ion exchange chromatography as described previously.[23] Briefly, the procedure was as follows:

Luria Bertani (LB) medium containing 50mg/ml carbenicillin was supplemented with the culture of *E. coli* Tuner (DE3) cells (Novagen) harbouring the expression plasmid pOPT_LPGpET22b and the prepared culture was incubated at 37 °C with continuous shaking until the culture reached an OD600 of 0.7–1.0. The temperature of the incubated culture was reduced to 20 °C and synthesis of the protein was induced by the addition of 0.2 mM isopropyl β-D-thiogalactoside (IPTG). After 4 h of induction, the cells were harvested by centrifugation and stored at -20 °C until further usage.

The stored cells were resuspended in ice-cold lysis buffer (25 mM Tris–HCl, pH 8.0, 100 mM NaCl, 1.25 mM EDTA and 0.05% Tween 20), and the cells were ruptured by three passages through a French pressure cell, then centrifuged to remove the debris formed and filtered to obtain a clear solution. The resulting protein extract was then loaded onto a HiTrap Q anion exchanger column (5 ml) which was previously equilibrated with the milliQ water and

suitable buffer (25 mM Tris–HCl, pH 8.0, supplemented with 100 mM NaCl), followed by a series of washing of the column with the buffer solution. The washings were collected and stored. The major fraction found to contain LPG (see below for the procedure used to detect the presence of LPG) was then loaded onto a 5 ml HiTrap SP cation exchanger column which was previously equilibrated with the 25 mM Tris–HCl, pH 8.0, supplemented with 100 mM NaCl. The column was then given a series of washings with the same buffer with different molar concentrations of NaCl (100 mM, 150 mM, 200 mM, 250 mM) and the washings were collected and stored under ice. It was observed that, of all the fractions collected, LPG was found to be eluted in 150 mM NaCl along with buffer and the major fractions of it were eluted with 25 mM Tris–HCl, pH 8.0, supplemented with 200 mM NaCl. Detection of the fractions containing LPG was done on a NuPAGE 4–12% Bis–Tris Gel (Invitrogen) by SDS-PAGE and staining with Coomassie Brilliant Blue. Fractions containing LPG were concentrated in 25 mM Tris–HCl, pH 8.0, 100 mM NaCl using an Amicon Ultra-15 centrifugal filter (10 kDa cut-off, Millipore). Protein concentration was then measured on a Thermo Scientific *NanoDrop* 2000 spectrophotometer and samples were snap frozen and stored at -80 °C for subsequent use.

Figure 3.1 clearly shows a prominent spot of protein near the 40 K region, in the lane corresponding to the fraction resulting from elution with 25 mM Tris–HCl, pH 8.0, supplemented with 200 mM NaCl washing.

Using this procedure 5 mg of LPG was obtained.

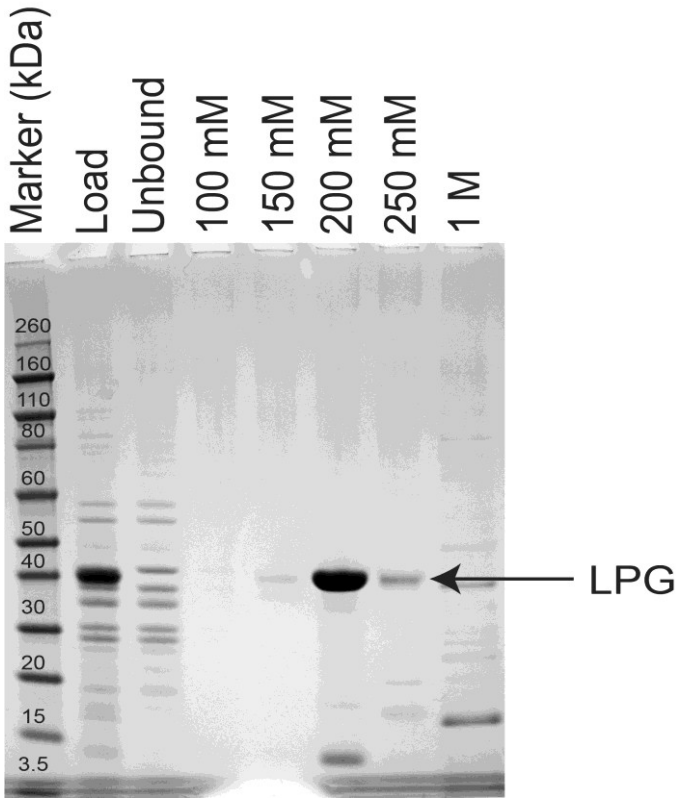

Figure 3.1: Gel Electrophoresis image of the sample of LPG expressed and purified in this work, containing various fractions following the purification protocol in different lanes. The first lane is the protein marker which has different marking standards based on the molecular weight followed. Moving left to right, the next lane shows the load fraction (crude material prior to clean-up), then unbound fraction, 100 mM NaCl washing, 150 mM NaCl washing, 200 mM NaCl washing, 250 mM NaCl washing and finally the 1 M NaCl buffer.

3.8 Conjugation of LPG and PG with AlexaFluor488

The conjugation of linker protein G (LPG) with Alexa Fluor 488 NHS involved series of steps. Purified LPG (Section 3.7) was first buffer exchanged with sodium bicarbonate buffer (pH adjusted to 8.5 with sodium hydroxide). After exchanging in suitable buffer (see below), the protein was then conjugated with the dye in suitable molar ratio with suitable buffer (0.1 X PBS). The recovery of the protein, the molar concentration of protein and also the degree of labelling of protein with the dye was also calculated. From the above calculations, the concentration of the different protein samples used were normalised to an equivalent value and were used in suitable ratio with the antibody for imaging the cells under the microscope. As a comparison for the method, the commercial protein G (purchased from Sigma) was also used. The detailed procedure of the conjugation of protein is detailed below.

3.8.1 Preparation of Reagents for Conjugation Work

100 mM sodium bicarbonate buffer (pH 8.5)

Sodium bicarbonate (1.68 g) was dissolved in milliQ water (200 mL) and the pH of the solution was adjusted to 8.5 using sodium hydroxide and filtered through a 0.45 μm filter.

0.1X PBS (Phosphate-Buffered-Saline)

One pellet of PBS was dissolved in milliQ water (200 mL) and stirred well. From this solution, 20 mL was taken and diluted to 200 mL with milliQ water to give 0.1X PBS and filtered through a 0.45 μm filter.

Microscopy

The bright field imaging of the cells was performed on an Olympus BX51 fluorescence microscope with a UPLSAPO 100 X oil immersion objective lens. Colour images of cells were captured on an Olympus 12.8 megapixel DP72 camera with a sensor resolution of 4140 x 3096.

3.8.2 Buffer exchange and normalization of protein concentration

100 μg of LPG (MW 30,504 g/mol, 100 μg/μL) was taken and passed through Sephadex G-25 column equilibrated with 100 mM sodium bicarbonate buffer (pH 8.5) and eluted using the same buffer. The fractions were collected and concentrated to 275 μL using an Ultra centrifugal filter (3 kDa cut-off, Millipore). The percentage recovery of the protein after buffer exchange was calculated using a NanoDrop UV spectrometer at 280 nm, and was found to be 42%. The procedure was repeated for protein-G (MW 21,600 g/mol) and the corresponding recovery was calculated as 86%. After calculating the recovery of the proteins, the concentration of the proteins were normalised (by taking the appropriate volumes of solution and diluting to a total volume of 300 μL with sodium bicarbonate solution (100 mM)), so as to obtain a valuable comparative result. The relevant data used in the normalisation are listed in Table 3.1. (Alexa488 NHS MW 647 g/mol)

Table 3.1: Data used for the normalisation procedure of protein G and LPG after buffer exchange.

Protein	Volume of Protein (μL)	Amount of protein in nmol	μL of Alexa 488NHS (1 mg/mL)	μL of Sodium bicarbonate buffer	Total volume (μL)	Protein to dye mole ratio
Protein-G	105	1.4	9 (14 nmol)	186	300	1:10
LPG	275	1.4	9 (14 nmol)	16	300	1:10

3.8.3 Conjugation of Proteins with Alexa Fluor 488 NHS

Based on the values mentioned in Table 3.1, the protein and the dye, along with buffer solution was added, mixed and protected from light and incubated at 37 °C for 1 h. The mixture was then passed through a Sephadex G-25 column, previously equilibrated with 0.1X PBS. After loading the sample into the column, a visible coloured band was evident and the column was eluted with the same buffer and only the visible coloured fractions were collected and stored; these fractions contained the protein-dye conjugate. The coloured fractions were mixed together and concentrated to 100 μL using an Ultra centrifugal filter (3 kDa cut-off, Millipore). The concentrated fractions were examined in using NanoDrop UV spectrometer and the absorbance maximum 280 nm (absorbance due to the protein component of the conjugate) and 494 nm (absorbance due to Alexa Fluor 488) was measured.[29] The sample reading was performed in triplicate to check the correctness of the value. The UV profiles of the LPG and PG-Alexa 488 conjugates are shown in Figures 3.2 and 3.3, respectively.

Table 3.2: Absorbance maximum values obtained, at 280 nm (A_{280}) and 494 nm (A_{494}), for the fractions believed to contain the desired conjugates

Sample Number	Protein-G		LPG	
	A_{280}	A_{494}	A_{280}	A_{494}
1.	0.018	0.044	0.033	0.173
2.	0.017	0.045	0.022	0.165
3.	0.016	0.047	0.046	0.164

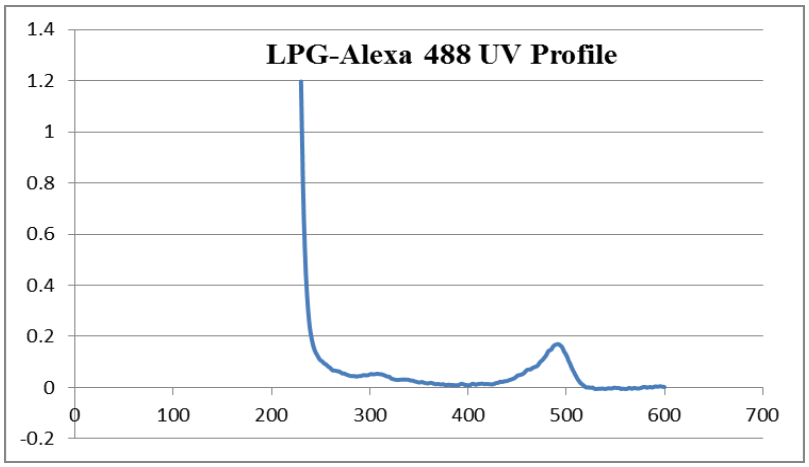

Figure 3.2: UV absorbance profile of LPG-Alexa 488 conjugate.

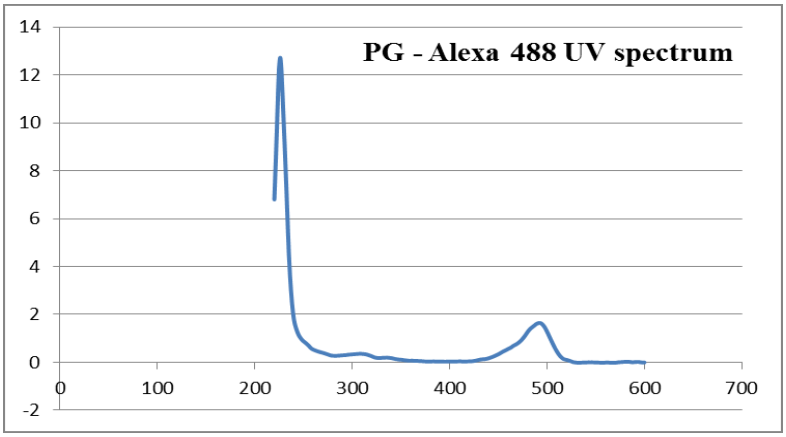

Figure 3.3: UV absorbance profile of PG-Alexa 488 conjugate.

3.8.4 Determination of protein concentration and degree of labelling

The conjugated protein concentration can be calculated using the formula:[29]

Protein Concentration (M) = $[A_{280} - (A_{494} \times 0.11)] \times$ dilution factor / molar extinction coefficient of Protein.

By applying the obtained values in the above mentioned formula, the concentration of protein in the synthesized LPG-488 and PG-488 conjugates were determined to be 5.11×10^{-7} M in 150 µL for LPG-488, and 4.4×10^{-7} M in 130 µL for PG-488.

Using the molar concentration of protein obtained from the above formula, the moles dye per mole protein was calculated using the formula:[29]

Moles dye per mole protein = A_{494} x dilution factor / 71,000 x protein concentration (M)

Where 71,000 is the molar extinction coefficient of Alexa 488 at 494 nm.

Substituting the values obtained for the corresponding PG and the LPG conjugates in the above mentioned formula gave the following values, For PG it was 1.41 mole of dye per mole of protein G and for LPG it was 4.7 mole of dye per mole of LPG.

3.8.5 Commercial Protein-G-Alexa Fluor 488 conjugate

To perform a comparative study with the conjugated protein-G and the linker protein-G (LPG), commercially available protein-G with Alexa 488 conjugate was also purchased to perform the imaging studies. This would not only serve as comparative study but also to check and evaluate the conjugates prepared and adds strength as a supporting document for the thus prepared conjugation protocol. The purchased protein-G Alexa conjugate (1 mg) was dissolved in 0.1X PBS (1 mL) and was divided into aliquots of 25 µL and stored at -20 °C until further use. The reported moles dye per protein ratio for the commercial protein-G conjugate was 2:1. This was also cross checked using the above mentioned formula for checking the moles dye per mole protein formula, which proved to be in agreement with the label claim. This result adds confidence to the calculations performed for the synthesized conjugates of protein-G and LPG.

3.9 Dynabead Experiment

10µL of the magnetic particles (Dynabeads) were taken and centrifuged to remove the supernatant. To this was added 200 µL of 0.1X PBS, mixed well and centrifuged and the supernatant was discarded. This procedure was repeated twice. Then to the magnetic particles was added 20 µL of the PG conjugate shaken well and mixed in a 360° rotating mixer for 10 minutes. Then the mixer was centrifuged and washed with 100 µL of 0.1X PBS twice and the obtained mixture was diluted to 20 µL with 0.1X PBS and was observed in the microscope for any visible fluorescence in the beads.

This experiment was performed for the each of three conjugates, the LPG-488 conjugate, the prepared PG-488 conjugate and the commercial PG-Alexa 488 conjugate. The images (not shown here) for conjugates were checked and it was observed that only in the case of the commercial PG-488 conjugate was some fluorescence observed. From these observations it

may be concluded that the binding of the synthesized protein-488 conjugates to the antibody was affected.

4.1 References

[1] J. Zimmermann, A. Zeug, B. Roder, *Phys. Chem. Chem. Phys.* **2003**, *5*, 2964-2969.

[2] M. Mao, X. S., J. Li , Y. Zou, R. Zhang, J. Pan, F. Dan, K. Zou, T. Yi, *Tetrahedron* **2012**, *68*, 5037-5041.

[3] C. Grunwald, K. Schulze, G. Giannone, L. Cognet, B. Lounis, D. Choquet, R. Tampe, *J. Am. Chem. Soc.* **2011**, *133*, 8090-8093.

[4] J. Lakowicz, *Principles of Fluorescence Spectroscopy*, 3rd ed., Springerlink, **2006** p.64.

[5] J. Lakowicz, *Anal. Biochem.* **2001**, *298*, 1-24.

[6] J. Lakowicz, *Principles of Fluorescence Spectroscopy*, 3rd ed., Springerlink, **2006** p.1-2.

[7] S. Sakamoto, F. Taura, B. Pongkitwitoon, W. Putalun, R. Tsuchihashi, J. Kinjo, H. Tanaka, S. Morimoto, *Anal. Bioanal. Chem.* **2010**, *396*, 2955-2963.

[8] M. Mao, S. Xiao, J. Li, Y. Zou, R. Zhang, J. Pan, F. Dan, K. Zou, T. Yi, *Tetrahedron Lett.* **2012**, *68*, 5037-5041.

[9] H. Kee, C. Kirmaier, L. Yu, P. Thamyongkit, J. Youngblood, M. Calder, L. Ramos, B. Noll, D. Bocian, R. Scheidt, R. Birge, J. Lindsey, D. Holten, *J. Phys. Chem. B.* **2005**, *109*, 20433-20443.

[10] W. Qin, M. Baruah, M. Auweraer, F. Schryver, N. Boens, *J. Phys. Chem. A* **2005**, *109*, 7371-7384.

[11] G. T. Morgan, R. B. Tunstall, *J. Chem. Soc., Trans.* **1924**, *125*, 1963-1967.

[12] J.-C. G. Bunzli, C. Piguet, *Chem. Soc. Rev.* **2005**, *34*, 1048-1077.

[13] G. Muller, *Dalton Trans.* **2009**, 9692-9707.

[14] S. Petoud, S. M. Cohen, J.-C. Bunzil, K. Raymond, *J. Am. Chem. Soc.* **2003**, *125*, 13324-13325.

[15] P. Ge, P. R. Selvin, *Bioconjugate Chem.* **2004**, *15*, 1088-1094.

[16] I. M. Clarkson, A. Beeby, J. I. Bruce, L. J. Govenlock, M. P. Lowe, C. E. Mathieu, D. Parker, K. Senanayake, *New J. Chem.* **2000**, *24*, 377-386.

[17] B. Alpha, J.-M. Lehn, G. Mathis, *Angew. Chem.* **1987**, *99*, 259-261.

[18] (a) J. Yuan, K. Matsumoto, *Anal. Chem.* **1998**, *70*, 596-601; (b) J. Yuan, G. Wang, H. Kimura, K. Matsumoto, *J. Inorg. Biochem.* **1997**, 429.

[19] (a) H. Zhang, L. Tian, R. P. Zhang, Z. Ye, J. Yuan, *Analyst* **2012**, *137*, 4502-4508; (b) L. Zhang, L. Tian, Z. Ye, B. Song, J. Yuan, *Tatanta* **2013**, *108*, 143-149; (c) L. Zhang, Y. Wang, Z. Ye, J. Dayong, J. Yuan, *Bioconj. Chem.* **2012**, *23*, 1244-1251.

[20] M. H. Petersen, S. A. Gevorgyan, F. C. Krebs, *Macromolecules* **2008**, *41*, 8986-8994.

[21] Q. Miao, J. Gao, Z. Wang, H. Yu, Y. Luo, T. Ma, *Inorg. Chim. Acta* **2011**, *376*, 619-627.

[22] D. C. G. A. Pinto, A. M. S. Silva, J. A. S. Cavaleiro, J. Elguero, *Eur. J. Org. Chem.* **2003**, 247-255.

[23] A. Sunna, F. Chi, P. L. Bergquist, *New Biotech.* **2013**, *30*, 485-492.

[24] R. M. McKinney, J. T. Spillane, G. W. Pearce, *J. Immunology* **1964**, *93*, 232-242.

[25] H. Ghafuri, *Current Chem. Lett.* **2014**, *3*, 183-188.

[26] Y. Zhao, V. Snieckus, *Org. Lett.* **2013**, *16*, 390-393.

[27] F. Akutsu, Y. Watanabe, M. Miura, K. Nagakubo, *Ploymer Commun.* **1983**, *24*, 213-215.

[28] H. Ishikawa, T. Sugiyama, K. Kurita, A. Yokoyama, *Bioorg. Chem.* **2012**, *41-42*, 1-5.

[29] Alexa Fluor® 488 Protein Labeling Kit. https://tools.lifetechnologies.com/content/sfs/manuals/mp10235.pdf.